Southeastern Geology: Volume 34, No. 2 May 1994

Editor in Chief: S. Duncan Heron, Jr.

Abstract

Academic journal published quarterly by the Department of Geology, Duke University.

SOUTHEASTERN GEOLOGY

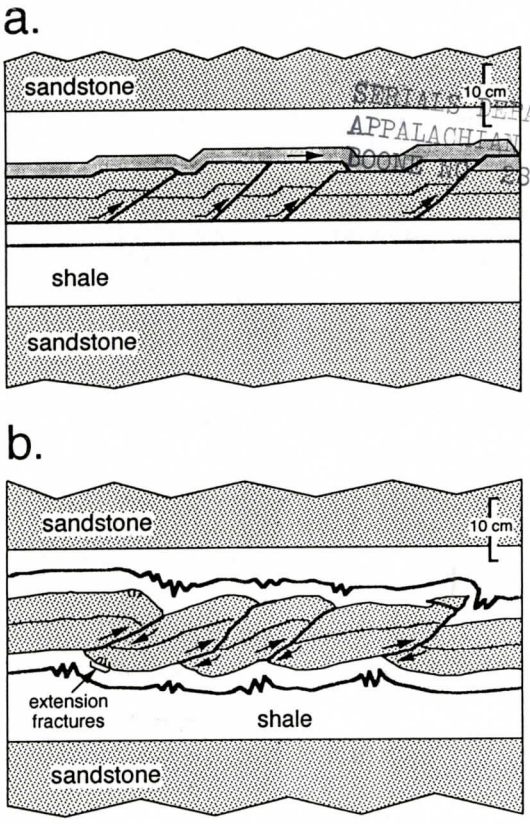

VOL. 34, NO. 2 MAY 1994

SOUTHEASTERN GEOLOGY

PUBLISHED

at

DUKE UNIVERSITY

Editor in Chief:

Duncan Heron

This journal publishes the results of original research on all phases of geology, geophysics, geochemistry and environmental geology as related to the Southeast. Send manuscripts to **DUNCAN HERON, DUKE UNIVERSITY, DEPARTMENT OF GEOLOGY, BOX 90233, DURHAM, NORTH CAROLINA 27708**. Phone 919-684-5321, Fax 919-684-5833, E Mail heron@rogue.geo.Duke.edu. Please observe the following:

1) Type the manuscript with double space lines and submit in duplicate.
2) Cite references and prepare bibliographic lists in accordance with the method found within the pages of this journal.
3) Submit line drawings and complex tables reduced to final publication size (no bigger than 8 x 5 3/8 inches).
4) Make certain that all photographs are sharp, clear, and of good contrast.
5) Stratigraphic terminology should abide by the North American Stratigraphic Code (American Association Petroleum Geologists Bulletin, v. 67, p. 841-875).

Subscriptions to *Southeastern Geology* per volume are: individuals - $15.00 (paid by personal check); corporations and libraries - $20.00; foreign $24. Inquires should be sent to: **SOUTHEASTERN GEOLOGY, DUKE UNIVERSITY, DEPARTMENT OF GEOLOGY, BOX 90233, DURHAM, NORTH CAROLINA 27708**. Make checks payable to: *Southeastern Geology.*

SOUTHEASTERN GEOLOGY is a peer review journal.

ISSN 0038-3678

SOUTHEASTERN GEOLOGY

Table of Contents

Volume 34, No. 2

May 1994

SOUTHEASTERN GEOLOGY
V. 34, No. 2, May 1994, p. 57-77

RHYTHMIC BEDDING IN THE PINE BARREN MEMBER OF THE CLAYTON FORMATION (LOWER PALEOCENE), ALABAMA

Richard A. Huchison, Jr.[1] and Charles E. Savrda

Department of Geology
Auburn University
Auburn, AL 36849-5305

ABSTRACT

The Pine Barren Member of the Clayton Formation in central Alabama and equivalent strata in western Alabama, which define the bulk of the highstand systems tract of a Lower Paleocene marine depositional sequence, are characterized by decimeter-scale rhythmic interbedding of sandy calcareous mudstones and fine-grained argillaceous limestones. Sedimentologic, ichnologic, and geochemical studies of this genetic package near Braggs, central Alabama, indicate that bedding couplets represent diagenetically enhanced dilution-scour-redox cycles. Mudstones were relatively oxygen-depleted substrates and were deposited during times of relatively high input of clastic sediments under at least periodically higher-energy conditions. Limestones accumulated during periods of quiescence and relatively low influx of terrigenous detritus, were relatively well-oxygenated substrates, and were later preferentially recrystallized at elevated temperatures associated with burial and/or under the influence of meteoric waters.

Reconnaissance of selected exposures at various other localities in western Alabama indicates that the thickness of the rhythmically bedded genetic package and the number of bedding couplets decrease from central to western Alabama, a pattern that is consistent with the interpretation of bedding couplets as prograding parasequences. In this context, the dilution-scour-redox cycles in the Pine Barren Member may have been modulated by short-term relative sea-level changes, short-term climate cycles, or a combination of both. Strong evidence implicating Milankovitch cycles as a modulating force is currently lacking.

INTRODUCTION

Cyclic sedimentation and rhythmic bedding have received considerable attention in recent years (e.g., Einsele and others, 1991). Much of this attention has been focussed on Cretaceous pelagic and hemipelagic chalk and marl sequences, which commonly exhibit decimeter- to meter-scale variations in carbonate content (e.g., Einsele, 1982; Arthur and others, 1984, 1986; Bottjer and others, 1986). Investigations of such rhythmites generally have emphasized the assessment of the paleoenvironmental cycles responsible and the external mechanisms that modulated cyclic environmental change.

Although carbonate cycles in many sequences have been enhanced to varying degrees by diagenesis (Ricken and Eder, 1991), most rhythmites do reflect a primary environmental signal (Fischer and others, 1985; Fischer, 1986). Rhythmites have been attributed to one or a combination of several environmental mechanisms, including dissolution cycles, dilution cycles, productivity cycles, redox cycles, and scour cycles (Arthur and others, 1986; Bottjer and others, 1986). These cyclic variations in paleoenvironmental parameters are most often ascribed to climate rhythms induced by cyclic changes in the earth's orbital parameters, i.e., the Milankovitch cycles (e.g., de Boer, 1982, 1991; Schwarzacher and Fischer, 1982;

1. Current address: Fox Environmental Services, Inc., 2501 Byington Beaver-Ridge Rd., Knoxville, TN 37931

de Boer and Wonders, 1984; Fischer and Schwarzacher, 1984; Fischer and others, 1985; Fischer, 1986, 1991). However, some carbonate cyclicity may be related to short-term relative sea-level dynamics that are independent of climate (e.g., King, 1990).

The Pine Barren Member of the Lower Paleocene (Danian) Clayton Formation in central Alabama and equivalent strata in western Alabama are characterized by a well-expressed, decimeter-scale interbedding of poorly indurated, sandy calcareous mudstones and indurated fine-grained argillaceous limestones. In the context of sequence stratigraphy, limestone-mudstone couplets in the Pine Barren previously have been interpreted to represent parasequences produced by short-term relative sea-level fluctuations (e.g., Vail and others, 1987). However, the nature of this rhythmic bedding has not been adequately documented and, hence, the causal mechanisms for depositional cyclicity have not been rigorously assessed. In order to evaluate this cyclicity and thereby better understand the physical and chemical conditions that prevailed on the Alabama shelf during the earliest Paleocene, we have undertaken sedimentological, ichnological, and geochemical studies of the Pine Barren rhythmites. In this paper we (1) describe the character of limestone/mudstone interbeds, (2) assess the role of various environmental and diagenetic parameters in the generation and/or accentuation of this rhythmic bedding, and (3) speculate on external driving mechanisms that may have modulated paleoenvironmental cycles.

STRATIGRAPHIC CONTEXT

The Clayton Formation is exposed in an arcuate belt that trends west-northwest across Alabama (Figure 1). The Clayton Formation lies unconformably upon Upper Cretaceous deposits and is overlain by the Paleocene Porters Creek Formation in most areas (Figure 1). The thickness, lithologic character, and age of the Clayton varies within the outcrop belt, reflecting both spatial changes in depositional environments (deepening to the west) and temporal fluctuations in relative sea-level (Gibson and others, 1982; Baum and Vail, 1988; Mancini and Tew, 1988, 1993).

In central Alabama, the Clayton Formation is divided into two members, both of which record marine shelf sedimentation. The basal Pine Barren Member consists of four informal units. These are, in ascending order: unit 1- thin (1 to 2 m), discontinuous sand bodies informally known as the "Clayton basal sands" (Mancini and others, 1989); unit 2- a thin (2 to 3 m) package of calcareous muddy sands and indurated, very sandy limestones; unit 3- a thick (~25 m) package of alternating sandy, calcareous mudstones and fine-grained limestones; and unit 4- several meters of densely fossiliferous sandy limestone referred to as the "*Turritella* rock." The upper McBryde Member, which is approximately 15 m thick, consists predominantly of chalky limestone with alternating well-indurated and poorly indurated beds (LaMoreaux and Toulmin, 1959).

Together, these two members contain two third-order depositional sequences (Baum and Vail, 1988; Mancini and Tew, 1988, 1993) (Figure 1). Using the terminology of Mancini and Tew (1993), these are sequences TAGC-1 and TAGC-2. Sequence TAGC-1, bounded at its base by a type 1 unconformity, includes the following components, in ascending order: incised-valley-fill deposits (unit 1); transgressive deposits with basal transgressive surface and upper surface of maximum starvation (unit 2); and highstand deposits (unit 3). Sequence TAGC-2, bounded at its base by a type 2 unconformity, includes in ascending order: shelf-margin deposits (unit 4); transgressive deposits with condensed section and surface of maximum starvation (McBryde Member); and highstand deposits (lower part of Porters Creek Formation). The rhythmically bedded interval addressed in this study defines a single genetic package-- the highstand systems tract of depositional sequence TAGC-1.

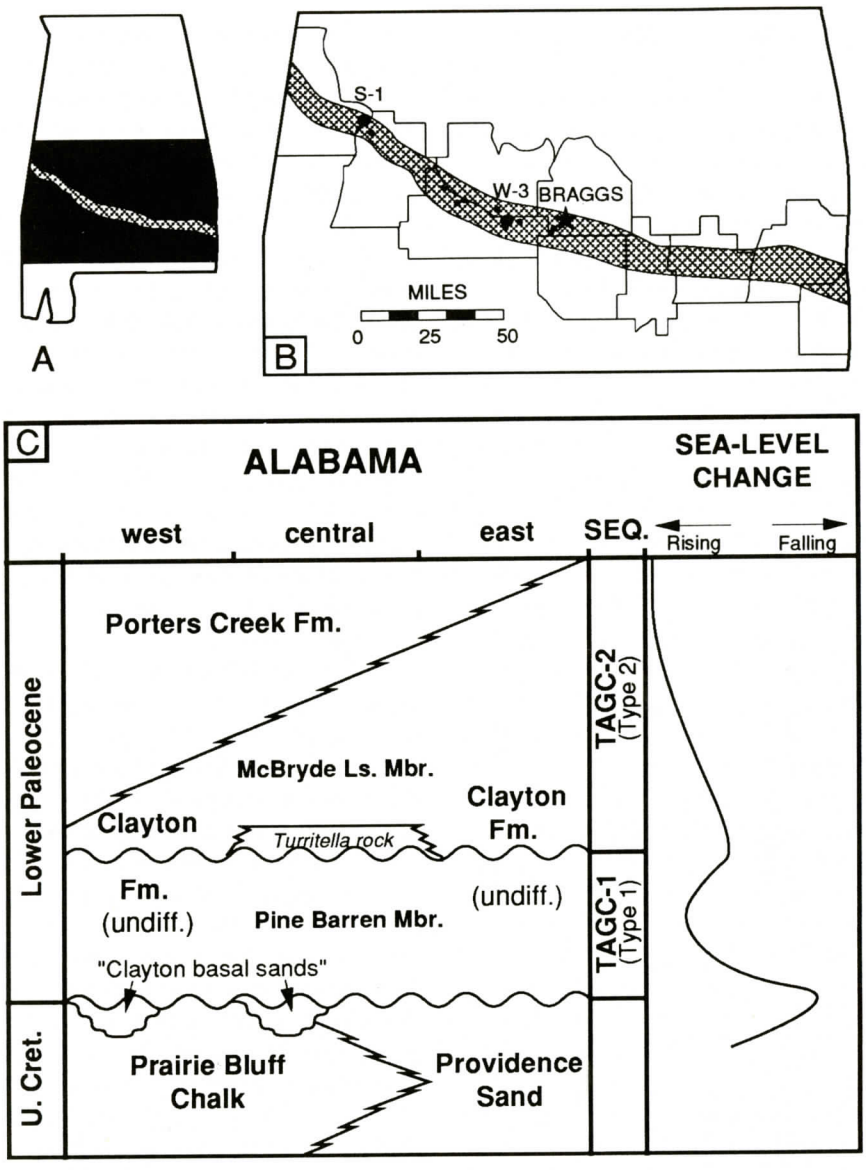

Figure 1. A,B) Distribution of Lower Paleocene strata (patterned) and study localities in western Alabama. B, an enlargement of black area in A, shows locations of Braggs, W-3, and S-1 sections in Lowndes, Wilcox, and Sumter Counties, respectively, and of additional sections of the Pine Barren Member reconnoitered in this study (small dots). C) Generalized lithostratigraphy and interpreted sea-level history for lowermost Paleocene strata in Alabama. Generalized sea-level curve is after Vail and others (1987). Sequence (SEQ.) terminology is after Mancini and Tew (1993). The rhythmically bedded package addressed in this study corresponds to the highstand systems tract of sequence TAGC-1.

METHODS

Our investigations emphasized detailed analysis of a well- exposed, nearly complete section of the Pine Barren Member near Braggs, central Alabama, but also included reconnaissance studies of equivalent strata exposed at several other sites.

Braggs Section

The Braggs section is a composite section constructed from two vertically extensive road-cut exposures along Alabama Highway 263 in Lowndes County, south of Braggs (Figure 1). Subsection L-1, the base of which contains the K-T boundary and, hence, has been the subject of numerous investigations (e.g., Jones and others, 1987; Donovan and others, 1988; Mancini and others, 1989; Zachos and others, 1989), includes the lowermost 13 m of the rhythmically bedded highstand systems tract. Subsection L-3, which lies 2.3 km south of subsection L-1, includes the upper 15 m of the rhythmically bedded interval and the overlying *Turritella* rock (Figure 2).

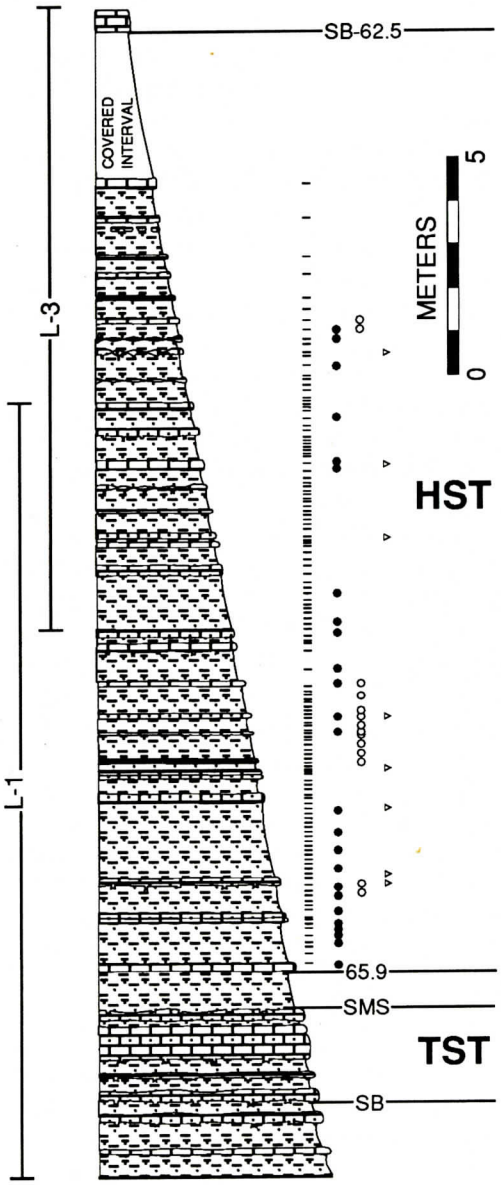

Figure 2. Generalized lithological column of the Braggs composite section of the Pine Barren Member exposed along Hwy 263, south of Braggs, central Alabama. Bars to the left of the column indicate relative stratigraphic content of subsections L-1 and L-3 (see text). Dashes, dots, open circles, and open arrows to the right of column indicate positions of samples for organic carbon/carbonate, thin-section, SEM, and stable isotopic analyses, respectively. SB= sequence boundary, SMS= surface of maximum starvation, TST= transgressive systems tract, and HST= highstand systems tract. Surfaces labeled 65.9 and 62.5 represent 65.9 ma NP1/NP2 nannofossil boundary (Jones and others, 1987) and 62.5 ma sequence boundary (from Vail and others, 1987), respectively.

After the two subsections were excavated, described and correlated, a continuous series of block samples representative of the entire genetic package was collected in order to better document in the laboratory differences among and between mudstones and limestones. Vertical slabs were cut from block samples to facilitate closer examination of primary and biogenic sedimentary fabrics. Selected slabs were then subsampled for carbonate and organic carbon analyses, thin section petrography, scanning electron microscopy, and carbon and oxygen isotopic studies of whole-rock carbonate (see Figure 2).

A total of 149 samples (~0.5 g) representing virtually all beds in the Braggs section were analyzed for carbonate and organic carbon. Carbonate contents were determined by weight loss after digestion in a 10% HCl solution and filtration through carbon-free borosilicate glass filters. Organic carbon contents were determined via analysis of insoluble residues using a LECO WR-12 thermal-conductivity carbon analyzer equipped with an automatic weight compensator. Precision levels for carbonate and organic carbon analyses are ± 0.5 and ± 0.02 weight percent, respectively.

Standard petrographic analyses of thin

sections prepared from 25 representative samples were performed to evaluate texture and composition of mudstones and limestones. Three hundred points were counted for each thin section. The mineralogy and long dimension were recorded for all encountered framework grains, herein defined as sedimentary particles of coarse-silt size (20 μm) or larger. Finer-grained primary or diagenetic material encountered at points in the interstices of framework grains was identified as clastic mud, carbonate micrite (or microspar), or cement. Additional observations on primary and diagenetic textures and components were made via examination of 8 samples under an ISI SS-40 scanning electron microscope.

Carbon and oxygen isotopic compositions of whole-rock carbonate in nine mudstone and seven limestone samples were analyzed at the Stable Isotope Laboratory at Texas A&M University. Subsamples weighing approximately 100 mg were acidified and the evolved CO_2 gas was analyzed on a Finnigan MAT 251 isotope ratio mass spectrometer. Values are reported in per mil notation relative to the PDB standard. Analytical precision is better than $\pm$0.1 per mil.

Reconnaissance of Additional Sections

Numerous other exposures of the Clayton Formation in Alabama were reconnoitered in an attempt to assess lateral variations in the rhythmically bedded genetic package. Because outcrops of the Clayton Formation east of the Braggs section apparently do not contain age-equivalent strata (Gibson and others, 1982), efforts were concentrated in western Alabama. All exposures examined in this part of the state are characterized by interbedded limestones and mudstones or marls. However, emphasis herein is placed on two sections-- section W-3 in Wilcox County and section S-1 in Sumter County (Figure 1)-- which, like the Braggs section, expose the genetic package in its entirety.

CHARACTER OF BRAGGS SECTION RHYTHMITES

General Section Description

A generalized lithologic column for the Braggs composite section is presented in Figure 2. The rhythmically bedded genetic package, from the basal surface of maximum starvation to the base of the superjacent *Turritella* rock, is 23 m thick. The lowermost 19.5 m of this interval contain 27 mudstone-limestone couplets with an average thickness of 71.5 cm (range= 26 to 198 cm) (Figure 3). The upper 3.5 m of the interval are weathered and/or covered, precluding the delineation of discrete bedding couplets. However, subtle terraces in the ground surface suggest that 4 to 6 additional couplets may be present therein.

Mudstones are the dominant component of each couplet and account for most of the variability in couplet thickness. Mudstone thickness ranges from 13 to 172 cm and averages 53 cm. Little variation among mudstones is apparent in the field-- all are olive gray to olive black, poorly indurated, silty to sandy, micaceous, calcareous, glauconitic, and macrofossiliferous (primarily bivalve molluscs).

Limestone beds are relatively thin, ranging from 7 to 34 cm (average= 18.5 cm). Nonetheless, they are rather conspicuous in outcrop owing to their greater induration and tendency to weather out as continuous ledges (Figure 3). Although the degree of induration varies slightly among limestone beds, they, like the associated mudstones, appear relatively uniform in the field. All are light olive gray, argillaceous, and fossiliferous. Contacts between limestones and mudstones range from planar to slightly undulatory and are generally sharp. However, bases of limestones are typically slightly more gradational than bed tops.

Sedimentary Fabrics

Observations of field exposures and slab surfaces demonstrate significant differences between mudstones and limestones with regard

Figure 3. Typical expression of interbedded mudstones and indurated limestones in Pine Barren Member, Braggs section. Outcrop is approximately 12 m in height.

to sedimentary fabrics.

Mudstones

Mudstones are generally highly bioturbated. Ichnofabrics are dominated by nondescript bioturbate background textures characterized by diffuse burrow mottling (Figure 4A). Recognizable discrete traces include only narrow, shallowly-penetrating, horizontal to subhorizontal, compacted burrows. Burrow boundaries are well-defined only where burrow fills contrast texturally with surrounding sediment. Identifiable ichnogenera include *Chondrites* (Figure 4A), the branches of which range from 2 to 3 mm in diameter, and larger-diameter (0.5 to 1.0 cm) *Planolites*. Both of these are traces of endobenthic deposit-feeding organisms of unknown affinity.

Although mudstones are heavily bioturbated, some vestige of primary sedimentary fabric is preserved within most beds. Remnant primary stratification features observed locally include discontinuous silt and sand laminae and thin (2 to 3 cm), parallel- to wavy-laminated sand lenses (Figure 4B).

Limestones

Limestones are thoroughly bioturbated and contain no primary internal stratification. Ichnofabrics are dominated by a homogeneous to burrow-mottled background upon which more discrete burrows are superimposed (Figure 4C). In contrast to mudstones, trace fossil assemblages are more diverse and include larger, less compacted, and better defined forms. The crustacean trace *Thalassinoides* dominates most limestones (Figure 4C). These large-diameter (1 to 3 cm), branching burrow networks are characterized by a strong vertical component and sharp burrow walls. Some *Thalassinoides* are filled, in part, with sandier sediments derived from overlying muds, indicating that the burrows remained open to the sediment-water interface for extended periods. Other recurring traces include *Chondrites*, *Planolites*, *Skolithos* (vertical, unbranched tubes), and, less commonly, vertical spreite structures assignable to the ichnogenus *Teichichnus*. The latter two burrow forms, which typically have diameters on the order of 1 cm, are produced by infaunal suspension feeders and deposit feeders, respectively.

Several of the limestones also represent the source beds for rare but unusually large-diameter (5 to 8 cm), vertically extensive *Thalassinoides paradoxicus* and, less commonly, *Gyrolithes* that penetrate downward as much as 1 m into underlying mudstones. Both of these forms have very sharp and ornamented (scratch-marked) walls, indicating production by crustaceans.

Carbonate and Organic Carbon

Data relating general lithology, carbonate, and organic carbon are summarized in Figure 5. Mudstones range from slightly to highly calcareous. Carbonate content generally falls

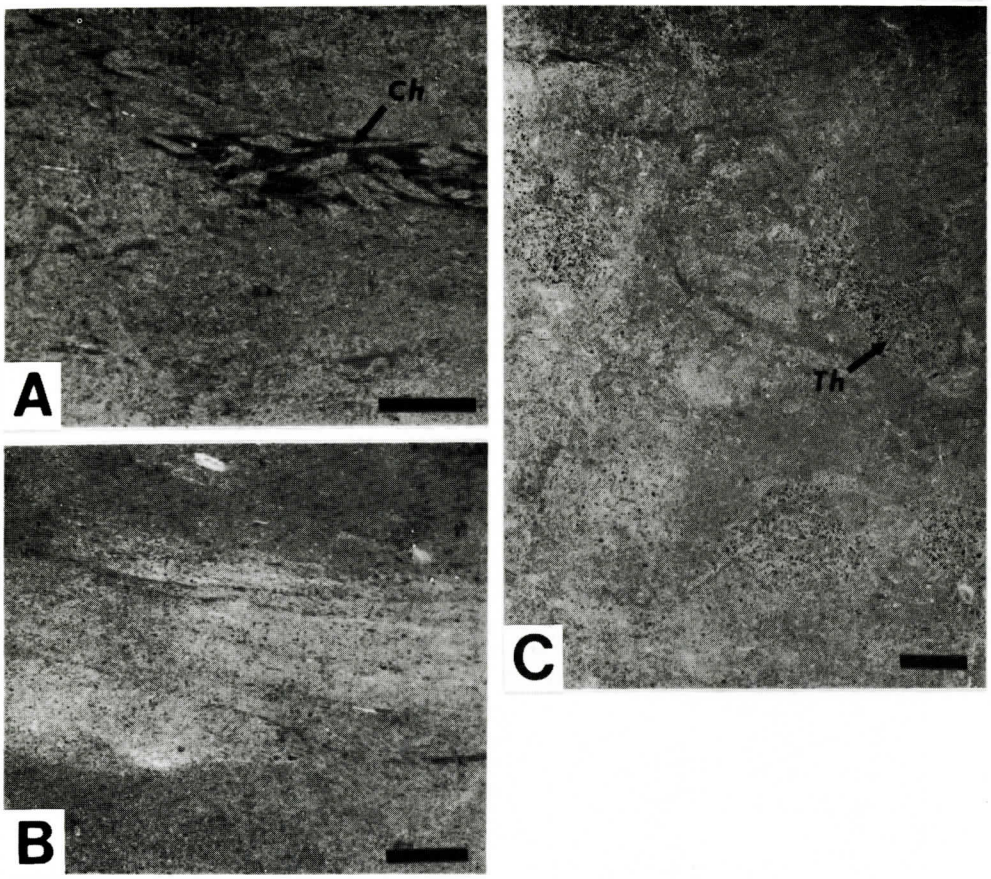

Figure 4. Typical ichnosedimentologic fabrics in mudstones (A and B) and limestones (C) of the Pine Barren Member, Braggs section. A) Burrow-mottled fabric typical of mudstones. Note small, better-defined *Chondrites* (Ch) in discontinuous clay-rich lens; B) Remnant silt and sand lamination in mudstone; C) *Thalassinoides* (Th)-dominated ichnofabric of limestones. Note relatively sharp burrow walls and low degree of compaction. Scale bars = 1 cm.

between 10 to 50% and averages 23%. A few samples have carbonate contents in excess of 50% and overlap with designated limestones (Figure 5). These aberrant samples likely reflect bioturbation and the resulting piping of carbonate-rich sediment from limestone bases downward into mudstones. With the exception of a few high-carbonate samples and a few deeply weathered low-carbonate samples, organic carbon contents of mudstones are relatively high. Most mudstones contain 0.4 to 1.4% (average= 0.9%) organic carbon.

Carbonate content of most beds designated as limestones falls between 65 to 80% (average= 71%). Organic carbon contents of limestones are uniformly low. With the exception of one sample, limestones contain less than 0.5% organic carbon. Average organic carbon content of limestones is 0.3% (Figure 5).

Petrography

The general petrographic characteristics of the mudstones and limestones are summarized below and in Figures 6 through 8. The reader is referred to Huchison (1993) for detailed data.

Mudstones

Mudstones (Figures 6A and 7A) can be divided into two textural components of

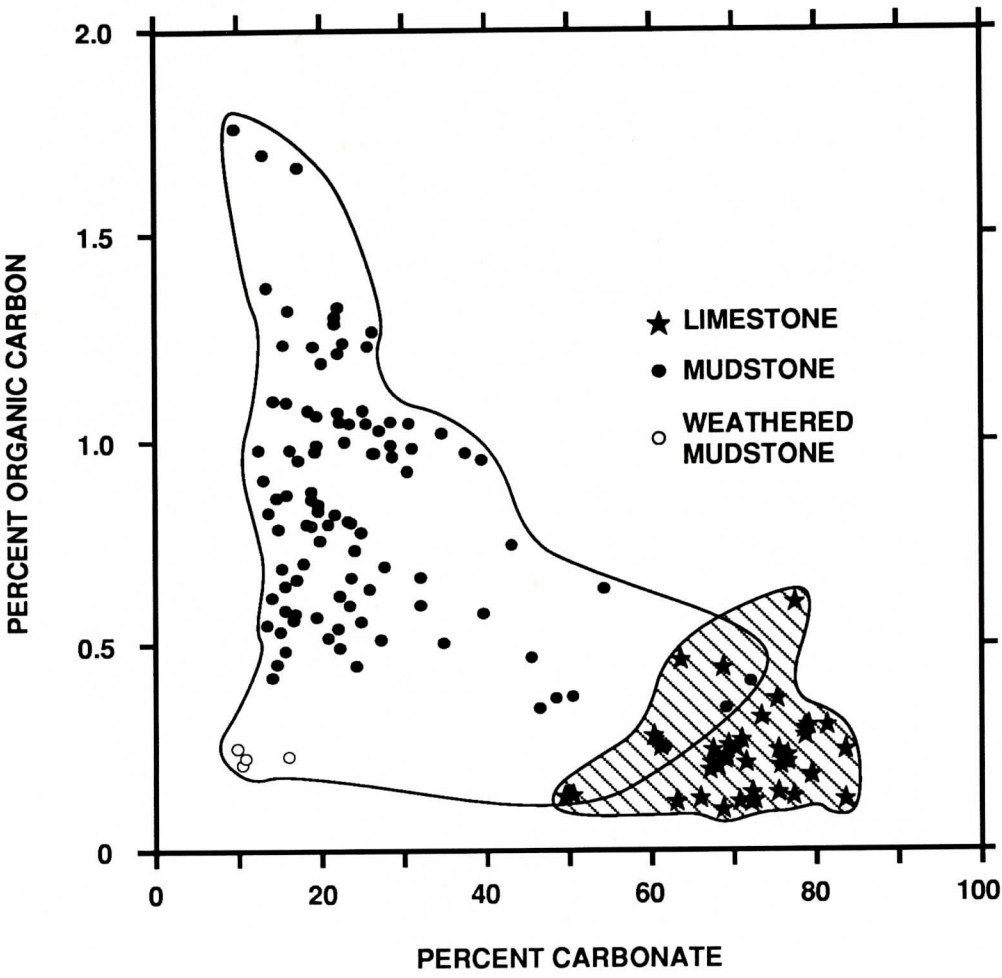

Figure 5.-Relations among organic carbon and carbonate contents and general lithology in the Braggs section.

roughly equal importance: 1) fine-grained mud matrix (clay- and fine silt-sized material); and 2) medium to coarse silt-, sand-, and pebble-sized grains. The mud matrix content of mudstones varies significantly from 33% to 76%, averaging approximately 55% (Figure 8A). Matrix is dominated by clastic components; terrigenous and micritic carbonate matrix comprise approximately 49% and 6% of the average mudstone, respectively (Figure 8B). However, based on carbonate data described above, the contribution of micrite to the matrix as judged from thin section analysis is slightly underestimated, presumably due to difficulties in identifying mineralogical affinities of finer fractions.

Medium to coarse silt-, sand-, and granule- to pebble-sized grains comprise, on the average, approximately 14%, 30%, and <1% of the mudstones, respectively (Figure 8A). Major grain types represented in this coarser fraction are, in order of decreasing abundance; glauconite, mica (primarily muscovite), quartz, and skeletal allochems.

Micas (average= 12%, range= 4 to 23%) are evenly dispersed throughout mud matrices. However, glauconite grains (average= 12%; range= 1 to 33%), most of which are worn and

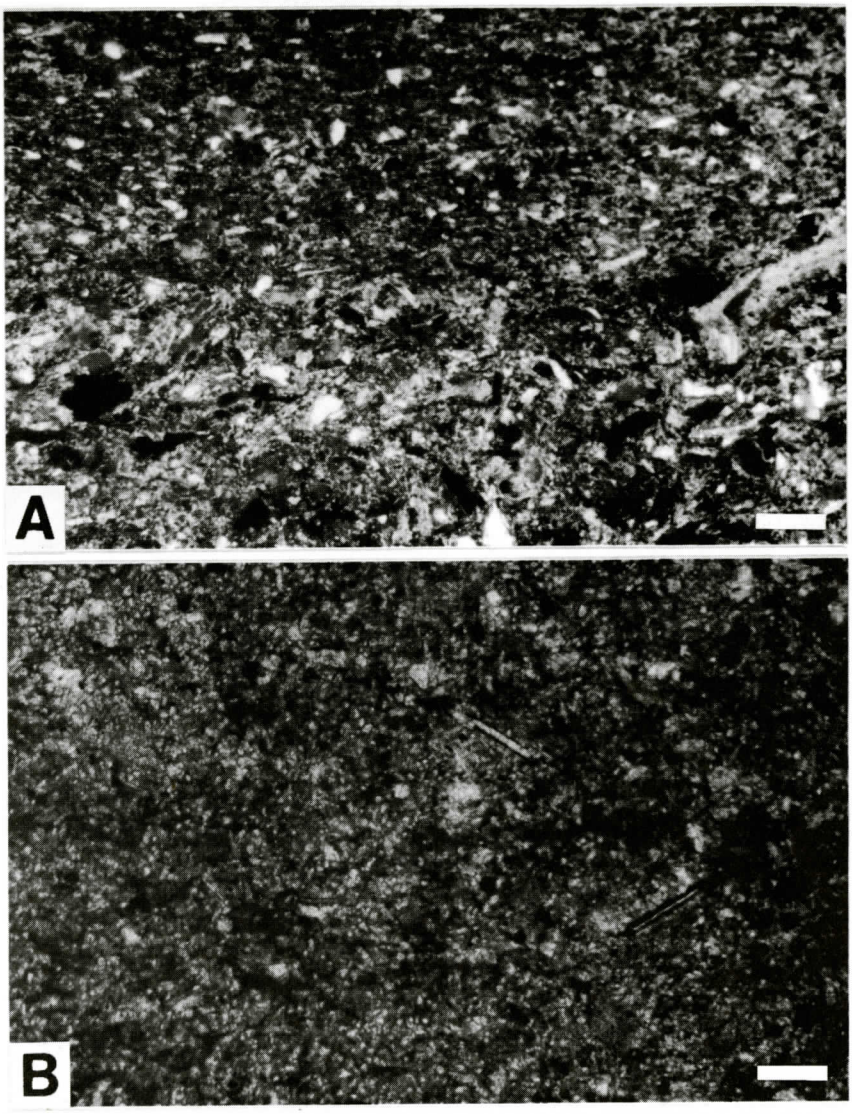

Figure 6.-Photomicrographs of typical silty to sandy mudstone (A) and limestone (B) from the Braggs composite section. Note concentrations of sand along laminae in A. B illustrates typical microspar textures resulting from recrystallization. Bar scales= 200 μm.

rounded and hence largely reworked, and quartz grains (average= 11%; range= 6 to 23%) are typically concentrated within irregular pods (burrow fills) and discontinuous lenses or laminae (Figure 6A). Skeletal carbonate allochems, which make up 2 to 14% (average= 7%) of mudstones, are primarily fragmented and include, in order of decreasing abundance; foraminifera, bivalves, gastropods, and echinoid spines.

Opaque grains, dominated by pyrite and its oxidized by-products, comprise 3% of the average mudstone (range= <1 to 9%), whereas feldspar, phosphatic grains, and intraclastic fragments represent minor components of the coarser silt- and sand-sized fraction (<1%).

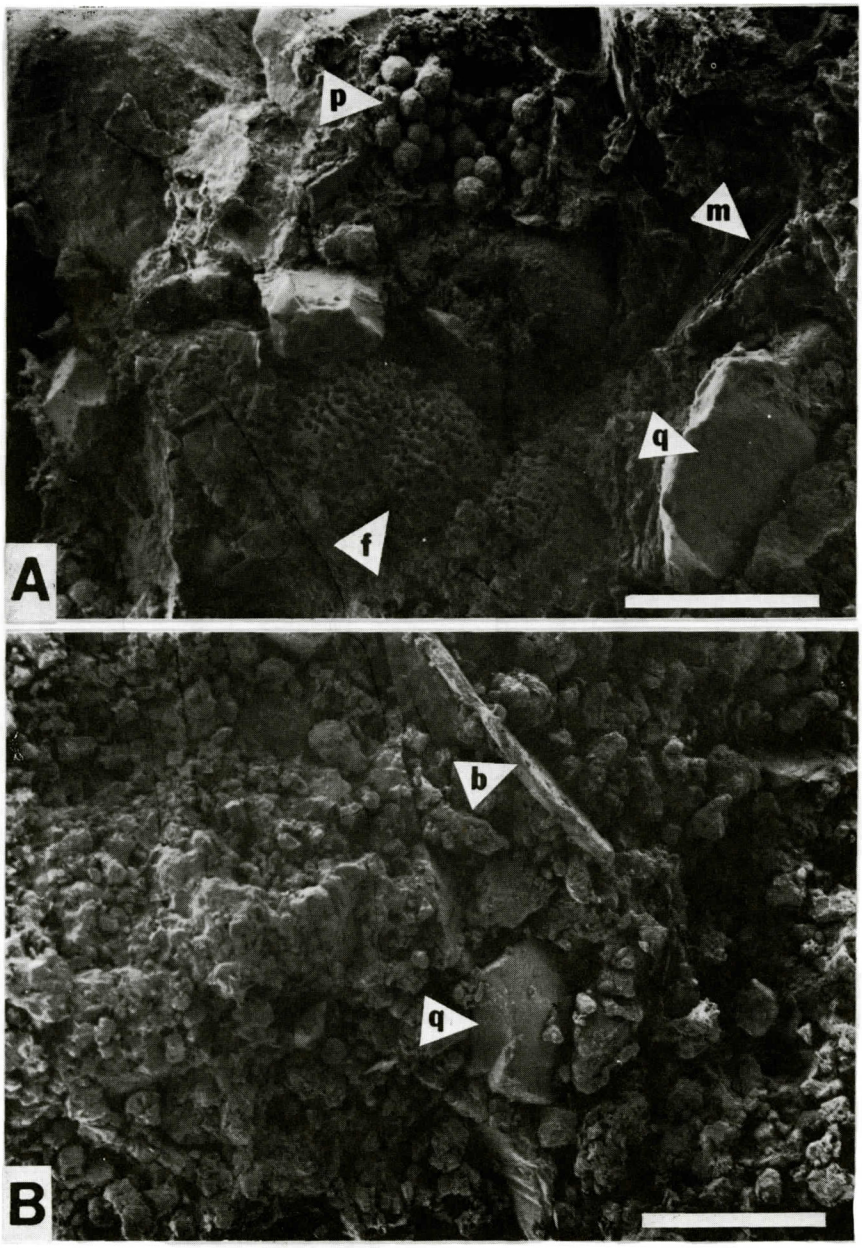

Figure 7.-Scanning electron photomicrographs of mudstone (A) and limestone (B) in Braggs section. Points p, q, f, m, and b designate pyrite, quartz, foraminifera, mica, and bivalve(?) fragments, respectively. Note lack of original depositional textures in limestone. Bar scale= 100 μm.

Limestones

Limestones (Figures 6B and 7B) are much finer grained than mudstones. Fine-grained mud matrix comprises 68 to 92% (average= 82%) of the limestones, whereas medium to coarse silt-, sand-, and granule- to pebble-sized grains make up the remainder (Figure 8A).

Carbonate analyses (see above) indicate that the contribution of clastics to the fine mud

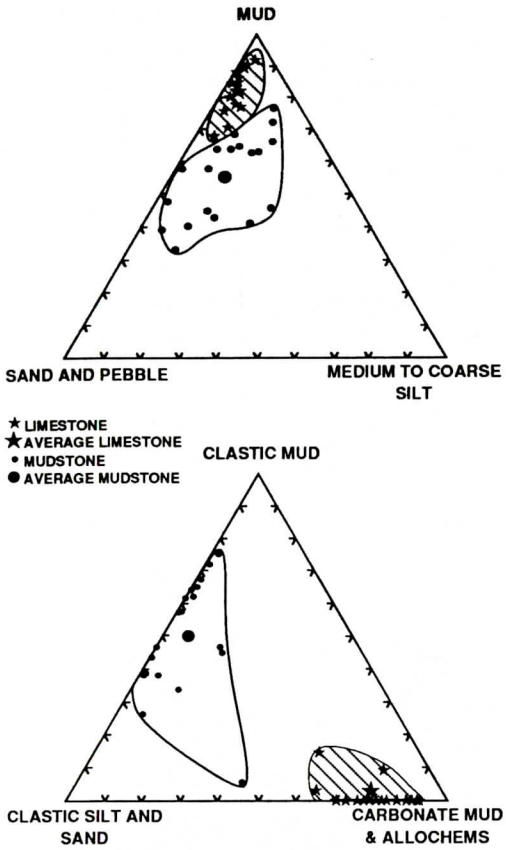

Figure 8. Textural and compositional parameters of mudstones and limestones in Braggs section. Although both lithologies are dominated by mud, mudstones are characterized by a larger coarse fraction (A). Moreover, composition of the mud-sized fraction in mudstones and limestones differ markedly (B).

fraction is underestimated by thin section analysis. However, as would be expected, this fraction is primarily calcareous (Figure 8B). In rare samples, the carbonate component is characterized by relatively unaltered micrite. However, for most limestone beds, textures are dominated by very finely to finely crystalline (5 to 25 um), low-Mg calcite microspar (Figures 6B and 7B).

Medium to coarse silt-, sand-, and granule- to pebble-sized grains comprise, on the average, approximately 4%, 14% and <1% of the limestones, respectively (Figure 8A). Major grain types represented in this coarser fraction are, in order of decreasing abundance; skeletal allochems, quartz, mica, and glauconite.

Carbonate skeletal allochems make up on average 7% of the limestones (range= 2 to 15%). Identifiable fragments represent the same fossil groups in roughly the same proportions as those recognized in mudstones. Quartz and glauconite grains, which represent 1 to 13% (average= 6%) and 0 to 11% (average= 2%) of limestones, respectively, are typically scattered throughout the carbonate matrix, but locally are concentrated in irregular pods that probably represent burrow fills. As in the mudstones, glauconite appears to be primarily detrital.

Mica grains are much less abundant, comprising only 1 to 6% (average= 2%) of the limestones. Fine to medium sand-sized opaque, phosphatic, and intraformational lithic grains similar to those in the mudstones occur in trace amounts (<1%).

Summarily, mudstones and limestones differ primarily with respect to the composition and amount of fine-grained constituents. In fact, the mudstone-limestone distinction is determined primarily by the composition of the mud-sized fraction (clastic vs. carbonate).

Stable Isotopic Compositions

Isotopic data, summarized in Figure 9, are generally consistent with those previously reported by Zachos and others (1989) for the basal part of the Pine Barren near Braggs. Oxygen isotopic ratios of the calcareous mudstones range from -1.98 to -2.96 per mil with an average of -2.36 per mil. Comparatively, all but one of the limestone samples are generally depleted by 1 to 2 per mil. Oxygen isotopic ratios of the limestones range from -2.29 to -4.16 with an average of -3.53 per mil.

No significant differences exist between mudstones and limestones with regard to carbon isotopic data. Carbon isotopic ratios range from 0.11 to 0.91 per mil (average= 0.54 per mil) and from -0.21 to 0.92 per mil (average= 0.36 per mil) for mudstones and limestones, respectively.

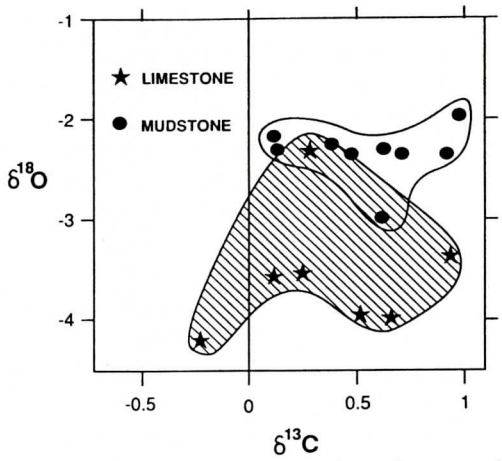

Figure 9. Oxygen versus carbon isotopic compositions of selected mudstone and limestone samples from Braggs section.

CHARACTER OF WESTERN ALABAMA SECTIONS

Generalized stratigraphic columns for sections W-3 and S-1 are shown in Figure 10.

Section W-3

The rhythmically bedded genetic package in section W-3, previously described by Lamoreaux and Toulmin (1959), is very similar to, albeit not as thick as, that in the Braggs section. Here the package is approximately 19.8 m thick and contains mudstone-dominated bedding couplets with an average thickness of 70 cm. On the basis of our reconnaissance field observations, the textures, compositions, and ichnosedimentary fabrics of mudstone and limestone interbeds are virtually identical to those in the Braggs section.

Section S-1

The genetic package in section S-1, previously described by Savrda (1991), differs from the Braggs and W-3 sections in several respects. In particular, the package is much thinner (3.6 m) and contains only 4 marl-limestone bedding couplets with an average thickness of 71 cm (Figure 10). Marls differ from their central Alabama mudstone counterparts in their higher carbonate contents (50 to 60%), their relatively lower organic carbon (0.6 to 0.7%) and sand contents, and the relative lack of remnant primary stratification features. Ichnofabrics are virtually identical, although marls also contain rare *Zoophycos* (Savrda, 1991).

Limestone interbeds in section S-1 bear a greater resemblance to their central Alabama counterparts. Carbonate contents range from

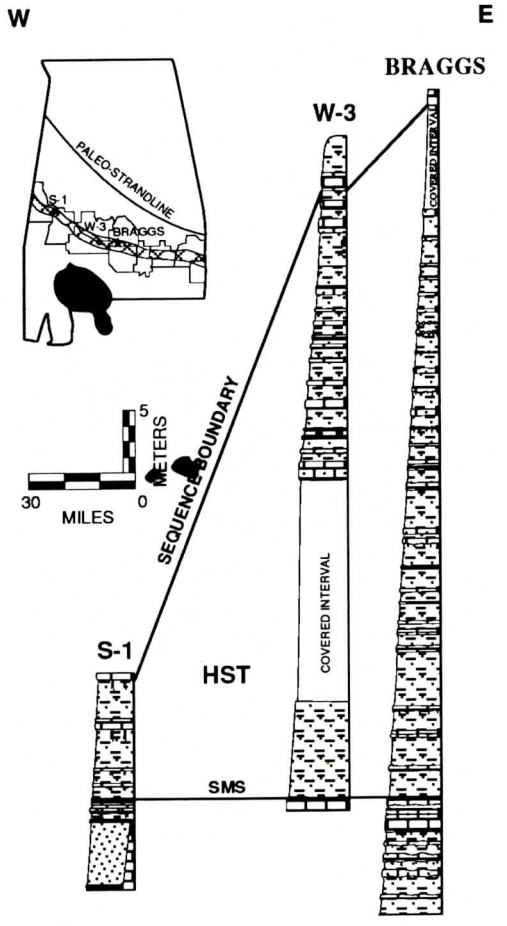

Figure 10. Generalized stratigraphic relationships between Braggs composite section and sections W-3 and S-1. Reduction in thickness of genetic package and the number of bedding couplets therein towards western Alabama (basinward) is consistent with the interpretation of bedding couplets as prograding parasequences.

70 to 80%, organic carbon contents range from 0.2 to 0.3%, and textures are micritic. Limestones also exhibit similar ichnofabrics, including deeply piped *Thalassinoides paradoxicus* (Savrda, 1991).

INTERPRETATION

Differences in texture, abundance of noncarbonate constituents, and sedimentary fabrics clearly indicate that limestone-mudstone cycles in the Pine Barren Member have a primary origin. However, evidence also attests to a diagenetic overprint that should be addressed before evaluating the environmental mechanisms responsible for depositional cyclicity.

Role of Diagenesis

Preferential diagenetic alteration of limestones is indicated by petrographic and isotopic data. The microspar textures that dominate the limestones are not primary but reflect recrystallization and associated aggradational neomorphism of originally micritic carbonate (Folk, 1965; Bathurst, 1971). This preferential recrystallization is also likely responsible for the oxygen isotopic differences between mudstones and limestones. Depleted oxygen isotopic values of the limestones relative to mudstones are difficult to explain by environmental causes alone. Isotopic differences could be interpreted to be the result of significantly greater influence by freshwater and/or elevated water temperatures (5 to 10 degrees higher) during deposition of the limestones. However, environmental changes of the required magnitude would necessitate changes in sea-level or climate that are unrealistic for this setting (Zachos and others, 1989). In contrast, the oxygen isotopic depletion of the limestones can be explained readily by diagenetic alteration at elevated temperatures associated with burial and/or under the influence of meteoric waters.

Reasons for preferential alteration of carbonate in the limestones are not clear. Mudstones and limestones may have differed with regard to the original mineralogy and, hence, diagenetic potential of carbonate micrite (i.e., micrite in carbonate-rich sediments may have been composed of a more reactive, metastable carbonate). Alternatively, micrite mineralogy of carbonate-poor and carbonate-rich sediments was originally the same but differences in amount and/or texture of noncarbonate components mediated selective diagenesis. For example, recrystallization of the carbonate-rich sediments may have been facilitated by the relative lack of reaction-inhibiting, Mg-bearing clays (Zachos and others, 1989). These and other potential causes of selective diagenesis cannot be adequately assessed without reliable data on the *original* mineralogy of carbonate micrite in both the mudstones and limestones.

Solution seams and stylolites indicative of rhythmic unmixing (i.e., solution transfer during burial diagenesis; see Einsele and others, 1991) are absent in the Pine Barren beds. Moreover, evidence for significant concretionary limestone growth (e.g., nodular geometries) is lacking. Hence, it is unlikely that preferential diagenesis has significantly enhanced the contrast in carbonate contents between limestones and mudstones. However, at the very least, recrystallization accentuated the carbonate rhythmicity by increasing the degree of induration of limestones and, consequently, the degree of differential erosion between the limestones and intervening mudstones. Unfortunately, this diagenetic overprint has masked primary sedimentary textures and isotopic signatures that could have been of potential use in the interpretation of the environmental mechanisms responsible for the carbonate cyclicity.

Primary Environmental Causes of Cyclic Sedimentation

As previously noted, rhythmic bedding in fine-grained carbonate sequences typically can be attributed to one or a combination of the following environmental mechanisms; dissolution cycles, scour cycles, redox cycles, productivity cycles, and dilution cycles (Arthur and others,

1986). The contribution of these cycle types to the Pine Barren rhythmicity is evaluated below, in the context of the Braggs section data.

Dissolution Cycles

Dissolution cycles are carbonate rhythms produced by cyclic changes in degree of saturation of marine waters with respect to calcium carbonate. Temporal variations in carbonate content produced by dissolution cycles are primarily developed in deeper-water settings where the sea floor lies between the carbonate compensation depth (CCD) and the lysocline (Fischer and others, 1985; Einsele and Ricken, 1991). Dissolution of carbonate is not inoperative altogether in shallow marine settings (Aller, 1982) and may be particularly extensive in relatively organic-rich sediments wherein decomposition of organic matter produces abundant CO_2 (Einsele and Ricken, 1991; Diester-Haass, 1991). However, dissolution cycles of the magnitude required to produce variations in carbonate comparable to that observed in the Pine Barren Member are generally not expected in shallow-marine shelf settings. On this basis alone, dissolution cycles can be discounted as the primary mechanism responsible for the Pine Barren carbonate rhythmicity.

Scour Cycles

Scour cycles are carbonate rhythms produced by periodic variations in bottom-current energy (Arthur and others, 1986). Originally defined on the basis of studies of Cretaceous chalks (Kennedy and Garrison, 1975), scour cycles in pelagic carbonates are typically expressed as alternations of normal chalk and omission surfaces, winnowed horizons, nodular chalks and/or hardgrounds. The chalks reflect normal deposition under low-energy conditions, whereas the latter features reflect higher-energy phases of erosion and/or nondeposition (Arthur and others, 1986). In the case of nodular chalks and hardgrounds, early carbonate cementation during depositional hiatuses resulted in diagenetic accentuation of carbonate rhythmicity (Kennedy and Garrison, 1975).

Our data indicate that carbonate cycles in the Pine Barren Member do coincide with variations in environmental energy. The finer grain size and lack of primary fabric in the limestones are indicative of consistently low-energy conditions. In contrast, aspects of sedimentary fabric and texture indicate that environmental energy was comparatively high, at least periodically, during mudstone deposition. The remnant sand laminae and lenses associated with the mudstones suggest periodic influence by storm waves or other bottom currents. Even where primary fabrics are absent, variability in energy levels is indicated by the admixture of fine and coarse components in these beds. Coarse silt- and sand-sized quartz, glauconite, and some skeletal allochems were likely introduced or concentrated during storm or winnowing events and subsequently mixed with finer muds and micas (hydrodynamically fine) via bioturbation.

Additional evidence for episodes of current intensification and winnowing is derived from ichnofabrics and their implications regarding substrate consistency. Diffuse burrow boundaries and high degree of burrow compaction indicate that mudstone substrates were normally rather fluid (soft to soupy). However, the *Th. paradoxicus* and *Gyrolithes* that pipe downward into mudstones from some limestones reflect the *Glossifungites* ichnofacies, which is diagnostic of dewatered, semiconsolidated substrates (firmgrounds) (Pemberton and Frey, 1985). Superposition of these traces over resident soup- to softground ichnofabrics suggests that overcompacted mud substrates were periodically exhumed by erosion.

Although the carbonate cyclicity in the Pine Barren Member does correspond with variations in environmental energy, it is not likely that scour cycles *directly* influenced the carbonate contrast between interbeds as they have in some chalks. There is no evidence for extended omission surfaces and/or synsedimentary lithification in the rhythmically bedded interval. Limestones were not

hardgrounds; ichnofabrics indicate that soft-ground conditions were maintained during the entire time that these relatively carbonate-rich sediments were in reach of infaunal organisms. Furthermore, surfaces interpreted to represent extended phases of winnowing (e.g., shell lags) are also absent. It is possible that the inferred higher-energy regime associated with the mudstones resulted in the winnowing and preferential removal of fine-grained carbonate mud. However, mudstones contain abundant clay-sized clastic sediments that likely would have been equally susceptible to winnowing by currents. Hence, the coincident variations in energy and carbonate content are interpreted to be separate responses to the same environmental mechanism.

Redox Cycles

Redox cycles are sedimentary rhythms produced by fluctuations in the degree of benthic oxygenation (Fischer and others, 1985; Arthur and others, 1986; Bottjer and others, 1986). These are typically expressed as an alternation of highly bioturbated, organic-poor beds and less extensively bioturbated or laminated, organic-rich intervals. Although associated changes in sediment color and fabric typically strongly accentuate the visibility of rhythmicity, redox cycles do not typically exert a significant control on relative carbonate contents of interbeds. In fact, redox cycles generally occur coincidentally with dilution and/or productivity cycles (Arthur and others, 1984; Bottjer and others, 1986; Eicher and Diner, 1989).

Our observations suggest that the carbonate rhythms in the Pine Barren Member were accompanied by changes in benthic oxygenation. Following the models of Savrda and Bottjer (1991; Savrda, 1992), the low-diversity assemblage of small, shallowly-penetrating burrows in the mudstones likely reflects relatively low benthic oxygenation, whereas the greater diversity and size (diameter and vertical extent) of burrows in the limestones indicate relatively improved benthic oxygen conditions. This interpretation is supported by the pronounced inverse relationship between organic carbon and carbonate. However, as described below, trends in organic carbon distribution could reflect a variety of environmental parameters (e.g., sedimentation rate, productivity, etc.) aside from oxygenation.

The inferred variations in redox conditions could possibly reflect periodic changes in bottom-water oxygenation caused by regional changes in circulation or water-mass stratification. However, the Pine Barren redox cycles more likely reflect variations in *pore-water* oxygenation that were controlled by changes in the physical properties of substrates and their effects on endobenthic organisms (Savrda, 1991; Savrda and Bottjer, 1991).

Productivity vs. Dilution Cycles

Dilution and productivity cycles are carbonate rhythms produced by cyclic variations in the input of terrigenous sediments and rate of biogenic carbonate production, respectively. Variations of these types are the only remaining viable mechanisms to explain the significant carbonate differences between the Pine Barren interbeds. Dilution and productivity cycles are often difficult to distinguish, particularly for sequences wherein diagenesis has precluded the evaluation of relative abundance of productivity-sensitive microfossils (Arthur and others, 1984).

Although productivity fluctuations cannot be eliminated as a contributing factor altogether, dilution cycles are favored as the primary mechanism to explain the Pine Barren carbonate rhythmicity. Evidence for this interpretation is drawn from (1) magnitude of carbonate fluctuations, (2) organic carbon/carbonate relationships, and (3) textural attributes.

Carbonate data alone cannot provide definitive information on cycle origin. However, differences in clastic/carbonate ratios between mudstones and limestones may provide supporting evidence. The average ratio of clastic/carbonate components in the Braggs section mudstones is approximately 3:1. Generation of the limestones, which have an aver-

age clastic/carbonate ratio of 1:3, would require either: (1) a reduction of clastic sediment input to 1/9 of the "mudstone" levels (assuming carbonate input is constant); or (2) a 9-fold increase in carbonate input (e.g., via increased productivity; assuming clastic input is constant). Although the latter is not impossible, this would require nutrient-supply variations of unusually high magnitude. The former scenario, which invokes a dilution mechanism for the cyclicity, is more probable.

The inverse relationship between carbonate and organic carbon in the Pine Barren beds is a feature common to many rhythmite sequences (e.g., Savrda and Bottjer, 1994). This relationship may be attributed to one or a combination of the following factors: (1) mudstone deposition was accompanied by decreased benthic oxygenation levels and, hence, enhanced preservation of organic matter (Demaison and Moore, 1980; Pratt, 1984); (2) mudstones accumulated at a greater rate, thereby reducing the time available for biochemical degradation of organic material at or near the sediment-water interface (Muller and Suess, 1979); (3) mudstone deposition was accompanied by increased input of terrestrial organic matter; or (4) increased marine productivity occurred during mudstone deposition (Calvert, 1987). Evidence described above suggests that benthic oxygen levels were lower (at least in pore waters) during mudstone deposition. Hence, factor (1) was likely influential. Factors (2) and (3) cannot be excluded and, if they were operational, support a dilution-cycle origin for the limestone/mudstone alternations. Factor (4) also cannot be excluded altogether. However, if marine productivity was higher during deposition of mudstones, then productivity cannot be called upon to explain the carbonate variations.

Any mechanism proposed to explain the causes of carbonate fluctuations in the Pine Barren Member should also explain other differences between interbeds, particularly sediment texture. The mudstones are considerably coarser than the limestones, reflecting higher environmental energy levels. An increase in environmental energy is easier to cointerpret in the context of the dilution mechanism. That is, it is reasonable to expect an increased input of clastic sediments in response to periods of higher energy. Conversely, there is no clear or predictable link between increased energy levels and diminished productivity that would support the interpretation of the Pine Barren rhythms as productivity cycles.

Summary

The available evidence suggests that carbonate rhythmicity was controlled primarily by variations in the input of terrigenous clastic sediments onto the Pine Barren shelf. These variations appear to have been accompanied by variations in benthic oxygenation and environmental energy. Hence, bedding couplets in the Pine Barren Member represent combined redox-scour-dilution cycles. Minor variations in the biogenic productivity of carbonate and/or dissolution of carbonate also may have occurred, but if so they played a diminutive role in governing variations in carbonate.

Lateral Changes in the Genetic Package

Section S-1 in western Alabama differs from the central Alabama sections (Braggs and W-3) in a manner that is consistent with its deeper-water setting. The finer grain size and higher carbonate contents of the carbonate-poor components in section S-1 are commensurate with sedimentation in a quieter shelf environment removed from the effects of storms and further from sources of terrigenous detritus. Comparatively lower organic carbon contents of the marls may reflect improved benthic oxygenation. However, they also may be attributed to overall lower sedimentation rates, which would result in increased residence time and, hence, extended biochemical degradation of organic matter at or near the sediment-water interface.

The drastic westward reduction in both the thickness of the genetic package and the number of bedding couplets therein is consistent with the sequence stratigraphic paradigm.

Highstand systems tracts, characterized by progradational parasequences, generally thin basinward (Van Wagoner and others, 1988). The interpretation of bedding couplets in the Pine Barren Member as parasequences is addressed further below.

DISCUSSION

Potential Forcing Mechanisms

The causes of the combined redox-scour-dilution cycles in the Pine Barren Member cannot be established with certainty. Possible forcing mechanisms include cyclic climate changes and/or short-term relative sea-level fluctuations.

Climate Variations

The Pine Barren depositional cycles may be related to changes in the intensity and/or frequency of storms in the Paleocene Gulf coast region. In this scenario, periods of increased input of clastic sediments recorded by the mudstones may reflect times of intensified precipitation and run-off, whereas coincidental increases in environmental energy may reflect increased influence of storm-generated waves on the shelf. Conversely, micritic limestones may record relatively calmer and drier periods when precipitation, runoff, and clastic input were greatly reduced.

Similar climate cycles have been called upon to explain combined redox-dilution cycles recorded in limestone-marl sequences of the Cretaceous western interior (e.g., Pratt, 1984). Heavily bioturbated, organic-poor limestones in these sequences are attributed to periods of diminished run-off, whereas weakly bioturbated to laminated, organic-rich marlstones and shales are ascribed to wet episodes and associated increased runoff. Variations in redox conditions that occur in association with these Cretaceous carbonate rhythms are generally attributed to climate-controlled phases of intensification and deterioration of thermohaline stratification of the western interior seaway (e.g. Pratt, 1984). As previously noted, redox variations expressed in the Pine Barren Member need not reflect similar changes in oxygenation of the water column. Instead, they simply may reflect changes in pore-water oxygenation.

Sea-level Variations

As noted above, the overall thickness of the rhythmically bedded genetic package and the number of bedding couplets therein decrease from shallower-water sites in central Alabama to deeper-water sites in western Alabama. In this regard, the bedding couplets can be modeled as prograding parasequences within this highstand systems tract. Parasequences represent relatively conformable successions of genetically related beds or bedsets bounded by marine flooding surfaces, and are interpreted to reflect short-term changes in relative sea-level (Van Wagoner and others, 1988). The bedding couplets of the Pine Barren Member previously have been interpreted as the products of such high-frequency sea-level changes (Vail and others, 1987; Baum and Vail, 1988). In this scenario, the limestones would represent periods of short-term sea-level rise during which the supply of clastic sediments to the shelf was reduced (sediment starvation). Conversely, the mudstones would represent short-term stillstands or relative drops in sea-level during which the supply of clastic sediments to the shelf was renewed.

The mechanism(s) responsible for the hypothesized short-term relative sea-level changes are generally poorly understood. Glacio-eustacy certainly can modulate high-frequency sea-level fluctuations but was likely not influential during the early Paleocene. The build-up and relaxation of intraplate stresses (see Cloetingh, 1988; King, 1990) represents a potential causal mechanism. However, evidence implicating such a tectonic control in the Paleocene Gulf coastal region is currently lacking. We propose an alternative mechanism that involves the influence of climate changes and their effects on the relative supply of clastic sediments to the marine

realm. That is, the role of climate and sea-level dynamics in the production of the Pine Barren dilution cycles may be linked. The bedding couplets may represent sea-level controlled parasequences but the relative sea-level changes may have been controlled, in part, by the aforementioned climate cycles. During wetter periods, the alleged increased input of terrigenous sediments could have resulted in both the progradation of clastic sediments across the shelf and the seaward migration of the shoreline. During drier times, when clastic sediment input was reduced, subsidence may have outpaced sedimentation, resulting in the landward migration of the shoreline and, hence, magnified sediment-starvation on the Pine Barren shelf.

Role of Milankovitch Cycles

If climate cycles were the principal forcing mechanism, can they be linked to Milankovitch orbital parameters? In order to establish potential relationships with orbital cycles, durations of depositional cycles must compare favorably with the periods of orbital eccentricity (~100 ky), axial precession (~20 ky), and/or axial obliquity (~40 ky). A rough estimate of the duration of the cycles in the Braggs section can be made on the basis of unit thickness and age range. According to Jones and others (1987), the NP1/NP2 nannofossil zone boundary at 65.9 my occurs at the top of the lowermost limestone in the genetic package, whereas Vail and others (1987) recognize the base of the *Turritella* rock as the 62.5 my sequence boundary (Figure 2). If it is assumed that erosion associated with the formation of this type 2 sequence boundary was minimal, then the rhythmically bedded interval near Braggs represents approximately 3.4 my. Assuming that the entire interval contains 31 couplets (includes 5 couplets in the covered interval), the average duration of each cycle would be approximately 110 ky. This closely matches the 100 ky eccentricity cycle. However, establishment of a link between the Pine Barren rhythms and eccentricity (and/or other orbital parameters) is tenuous for the following reasons:

(1) Our estimate of average cycle duration is based on average couplet thickness (~71 cm). Considering the significant range in couplet thickness (26 to 198 cm), cycle durations may have been equally variable, ranging from 40 to 308 ky. This indicates that environmental changes may have been more episodic than periodic.

(2) More important, the estimated time represented by the rhythmically bedded interval in the Braggs section may be in error, owing to inaccuracies inherent in radiometric age determinations and/or significant section loss at or below the 62.5 ma sequence boundary. An average sedimentation rate of 9 mm/ky, calculated for the Braggs section assuming a 3.4 my duration and 40% compaction, is unusually low for clastic-dominated marine shelf settings (Schindel, 1980). Even when limestones, which represent approximately 25% of the section, are factored out (assuming that limestones accumulated 10 times slower than mudstones), the calculated mudstone accumulation rates are still unusually low (~27 mm/ky). This suggests that the section is stratigraphically incomplete, a conclusion that is not surprising when the aforementioned evidence for periodic winnowing and erosion is considered. Consequently, the signal of Milankovitch orbital parameters, if present at all, may be obscured beyond recognition.

CONCLUSIONS

(1) Comparative analyses of primary and biogenic sedimentary structures, sediment textures, and compositions indicate that rhythmic bedding in the Pine Barren Member is primarily the product of combined dilution-scour-redox cycles. Mudstones reflect times of relatively high input of clastic sediments, periodic influence by storm-generated and/or other currents, and the prevalence of relatively oxygen-depleted substrates. Intervening limestones reflect periods of relative quiescence,

slow accumulation of carbonate mud, and the development of oxygenated substrates. Limestones likely accumulated as biogenic ooze but postdepositional alteration has precluded an adequate assessment of the original constituents of the carbonate mud.

(2) Although the carbonate rhythmicity reflected by mudstone/limestone couplets reflects a primary environmental cyclicity, rhythmic bedding in the Pine Barren Member was enhanced by preferential diagenetic alteration of the limestones. Microspar textures and isotopic data indicate that limestones were recrystallized at elevated temperatures during burial diagenesis and/or under the influence of meteoric waters.

(3) The forcing mechanisms responsible for controlling environmental cycles during Pine Barren deposition cannot be determined with certainty. The apparent seaward reduction in both the thickness of the rhythmically bedded genetic package and the number of bedding couplets is consistent with models for highstand systems tracts wherein bedding couplets are interpreted as prograding parasequences (Vail and others, 1987; Baum and Vail, 1988). This implies that short-term sea-level changes may have modulated cyclic sedimentation. However, climate cycles, which could have influenced run-off, input of clastic sediments, and the relative frequency and/or intensity of storms, may have been the principle driving mechanism. Although climate cycles may have been important, currently there is no strong evidence to indicate that they were controlled by Milankovitch orbital rhythms.

ACKNOWLEDGMENTS

The bulk of this research was conducted as part of an MS thesis project by RAH. Partial support for this project was provided by a Grant-in-Aid from the Gulf Coast Association of Geological Societies (to RAH) and NSF grant EAR-9004923 (to CES). Comments and suggestions by Mitchell Malone helped improve the manuscript.

REFERENCES CITED

Aller, R.C., 1982, Carbonate dissolution in nearshore terrigenous muds: the role of physical and biological reworking: Journal of Geology, v. 90, p. 79-95.

Arthur, M.A., Dean, W.E., Bottjer, D.J., and Scholle, P.A.,1984, Rhythmic bedding in Mesozoic-Cenozoic pelagic carbonate sequences: The primary and diagenetic origin of Milankovitch-like cycles, *in* Berger, A., et al., eds., Milankovitch and Climate: Riedel, Dordrecht, p. 191-222.

Arthur, M.A., Bottjer, D.J., Dean, W.E., Fischer, A.G., Hattin, D.E., Kauffman, E.G., Pratt, L.M., and Scholle, P.A. (R.O.C.C. Group), 1986, Rhythmic bedding in Upper Cretaceous pelagic carbonate sequences: Varying sedimentary response to climatic forcing: Geology, v. 14, p. 153-156.

Bathurst, R.G.C., 1971, Carbonate Sediments and their Diagenesis: Developments in Sedimentology no. 12: Elsevier, New York, 658 p.

Baum, G.R., and Vail, P.R., 1988, Sequence stratigraphic concepts applied to Paleogene outcrops, Gulf and Atlantic basins, *in* Wilgus, C.K., et al., eds., Sea-level changes: An integrated approach, Society of Economic Paleontologists and Mineralogists, Special Publication no. 42, p. 309-327.

Bottjer, D.J., Arthur, M.A., Dean, W.E., Hattin, D.E., and Savrda, C.E., 1986, Rhythmic bedding produced in Cretaceous pelagic carbonate environments: Sensitive recorders of climatic cycles: Paleoceanography, v. 1, p. 467-481.

Calvert, S.E., 1987, Oceanographic controls on the accumulation of organic matter in marine sediments, *in* Fleet, A.J., and Brooks, J., eds., Marine petroleum source rocks, Geological Society of London, Special Publication No. 26, p. 137-151.

Cloetingh, S., 1988, Intraplate stresses: a cause for third-order cycles in apparent sea-level?, *in* Wilgus, C.K., et al., eds., Sea-level changes: an integrated approach, Society of Economic Paleontologists and Mineralogists, Special Publication No. 42, p. 19-30.

de Boer, P.L., 1982, Cyclicity and the storage of organic matter in Middle Cretaceous pelagic sediments, *in* Einsele, G., and Seilacher, A., eds., Cyclic and Event Stratification, Springer-Verlag, New York, p. 456-475.

de Boer, P.L., 1991, Pelagic black shale-carbonate rhythms:Orbital forcing and oceanographic

response, *in* Einsele, G., *et al.*, eds., Cycles and Events in Stratigraphy, Springer-Verlag, New York, p. 63-78.

de Boer, P.L., and Wonders, A.A.H., 1984, Astronomically induced rhythmic bedding in Cretaceous pelagic sediments near Moria (Italy), *in* Berger, A., *et al.*, eds., Milankovitch and Climate, Riedel, Dordecht, p. 177-190.

Demaison, G.J., and Moore, G.T., 1980, Anoxic environments and oil source bed genesis: American Association of Petroleum Geologists Bulletin, v. 64, p. 1179-1209.

Diester-Haass, L., 1991, Rhythmic carbonate content variations in Neogene sediments above the lysocline, *in* Einsele, G., *et al.*, eds., Cycles and Events in Stratigraphy, Springer-Verlag, New York, p. 94-109.

Donovan, A.D., Baum, G.R., Blechschmidt, G.L., Loutit, T.S., Pflum, C.E., and Vail, P.R., 1988, Sequence stratigraphic setting of the Cretaceous-Tertiary boundary in central Alabama, *in* Wilgus, C.K., *et al.*, eds., Sea-level changes-- an integrated approach, Society of Economic Paleontologists and Mineralogists, Special Publication No. 42, p. 299-307.

Eicher, D.L., and Diner, R., 1989, Origin of the Cretaceous Bridge Creek cycles in the western interior, United States: Palaeogeography, Palaeoclimatology, Palaeoecology, v. 74, p. 127-146.

Einsele, G., 1982, Limestone-marl cycles (perodites): Diagnosis, significance, causes- review, *in* Einsele, G., and Seilacher, A., eds., Cyclic and Event Stratification, Springer-Verlag, New York, p. 8-53.

Einsele, G., and Ricken, W., 1991, Limestone-marl alterations- an overview, *in* Einsele, G., *et al.*, eds., Cycles and Events in Stratigraphy, Springer-Verlag, New York, p. 23-47.

Einsele, G., Ricken, W., and Seilacher, A., 1991, Cycles and events in stratigraphy- Basic concepts and terms, *in* Einsele, G., *et al.*, eds., Cycles and Events in Stratigraphy, Springer-Verlag, New York, p. 1-19.

Fischer, A.G., 1986, Climatic rhythms recorded in strata: Annual Review of Earth and Planetary Science, v. 14, p. 351-376.

Fischer, A.G., 1991, Orbital cyclicity in Mesozoic strata, *in* Einsele, G., *et al.*, eds., Cycles and Events in Stratigraphy, Springer-Verlag, New York, p. 48-62.

Fischer, A.G., and Schwarzacher, W., 1984, Cretaceous bedding rhythms under orbit control, *in* Berger, A., *et al.*, eds., Milankovitch and Climate, Riedel, Dordrecht, p. 163-175.

Fischer, A.G., Herbert, T., and Premoli Silva, I., 1985, Carbonate bedding cycles in Cretaceous pelagic and hemipelagic sequences, *in* Pratt, L.M., *et al.*, eds., Fine-grained deposits and biofacies of the Cretaceous Western Interior Seaway: Evidence of cyclic sedimentary processes, Society of Economic Paleontologists and Mineralogists, Field Trip Guidebook Number 4, p. 1-10.

Folk, R.L., 1965, Some aspects of recrystallization in ancient limestones, *in* Pray, L.C., and Murray, R.C., eds., Dolomitization and limestone diagenesis, Society of Economic Paleontologists and Mineralogists, Special Publication no. 13, p. 14-48.

Gibson, T.G., Mancini, E.A., and Bybell, L.M., 1982, Paleocene to Middle Eocene stratigraphy of Alabama: Gulf Coast Association of Geological Societies Transactions, v. 32, p. 449-458.

Huchison, R.A., 1993, Character and origin of rhythmic bedding in the Pine Barren Member of the Clayton Formation, Lower Paleocene, Alabama: Unpublished Masters Thesis, Auburn University, 145 p.

Jones, D.R., Mueller, P.A., Bryan, J.R., Dobson, J.P., Channell, J.E.T., Zachos, J.C., and Arthur, M.A., 1987, Biotic, geochemical, and paleomagnetic changes across the Cretaceous/Tertiary boundary at Braggs, Alabama: Geology, v. 15, p. 311-315.

Kennedy, W.J., and Garrison, R.E., 1975, Morphology and genesis of nodular chalks and hardgrounds in the Upper Cretaceous of southern England: Sedimentology, v. 22, p. 311-386.

King, D.T.,Jr.,1990, Upper Cretaceous marl-limestone sequences of Alabama: Possible products of sea-level change, not climate forcing: Geology, v. 18, p. 19-22.

LaMoreaux, P.E., and Toulmin, L.D., 1959, Geology and ground-water resources of Wilcox County, Alabama: Alabama Geological Survey County Report no. 4, 280 p.

Mancini, E.A., and Tew, B.H., 1988, Paleocene sequence stratigraphy of southwestern Alabama: Gulf Coast Association of Geological Societies Transactions, v. 38, p. 453-460.

Mancini, E.A., and Tew, B.H., 1993, Eustacy versus subsidence: Lower Paleocene depositional sequences from southern Alabama, eastern Gulf Coastal Plain: Geological Society of America Bulletin, v. 105, p. 3-17.

Mancini, E.A., Tew, B.H., and Smith, C.C., 1989, Cretaceous-Tertiary contact, Mississippi and Alabama: Journal of Foraminiferal Research, v. 19, p. 93-104.

Muller, P.J., and Suess, E., 1979, Productivity, sedimentation rate and sedimentary organic matter in the oceans- I. organic carbon preservation: Deep-sea Research, v. 27A, p. 1347-1362.

Pemberton, S.G., and Frey, R.W., 1985, The *Glossifungites* ichnofacies: modern examples from the Georgia coast, U.S.A., *in* Curran, H.A., ed., Biogenic sedimentary environments, Society of Economic Paleontologists and Mineralogists, Special Publication no. 35, p. 237-259.

Pratt, L.M., 1984, Influence of paleoenvironmental factors on preservation of organic matter in Middle Cretaceous Greenhorn Formation, Pueblo, Colorado: American Association of Petroleum Geologists Bulletin, v. 68, p. 1146-1159.

Ricken, W., and Eder, W., 1991, Diagenetic modification of calcareous beds- an overview, *in* Einsele, G., *et al.*, eds., Cycles and Events in Stratigraphy, Springer-Verlag, New York, p. 430-449.

Savrda, C.E., 1991, Ichnology in sequence stratigraphic studies: an example from the Lower Paleocene of Alabama: Palaios, v. 6, p. 39-63.

Savrda, C.E., 1992, Trace fossils and benthic oxygenation, *in* Maples, C.G., and West, R.R., eds., Trace Fossils, Paleontological Society Short Course Notes No. 5, p. 171-196.

Savrda, C.E., and Bottjer, D.J., 1991, Oxygen-related biofacies in marine strata: an overview and update, *in* Tyson, R.V., and Pearson, T.H., eds., Modern and ancient continental shelf anoxia, Geological Society of London, Special Publication no. 58, p. 201-219.

Savrda, C.E., and Bottjer, D.J., 1994, Ichnofossils and ichnofabrics in rhythmically bedded pelagic/hemi-pelagic carbonates: recognition and evaluation of benthic redox and scour cycles, *in* de Boer, P., and Smith, D., eds., Orbital forcing and cyclic sequences, International Association of Sedimentologists, Special Publication no. 19, p. 195-210.

Schindel, D.E., 1980, Microstratigraphic sampling and the limits of paleontological resolution: Paleobiology, v. 6, p. 408-426.

Schwarzacher, W., and Fischer, A.G., 1982, Limestone-shale bedding and perturbations of the earth's orbit, *in* Einsele G., and Seilacher, A., eds., Cyclic and Event Stratification, Springer-Verlag, New York, p. 72-94.

Vail, P.R., Baum, G.R., Loutit, T.S., Donovan, A.D., Mancini, E.A., Tew, B.H., 1987, Sequence stratigraphy of the uppermost Cretaceous and Paleogene of the Alabama/western Georgia coastal plain, Field Trip Guidebook for the Lafayette Geological Society, p. 1-44.

Van Wagoner, J.C., Posamentier, H.W., Mitcham, R.M., Vail, P.R., Sarg, J.F., Loutit, T.S., and Hardenbol, J., 1988, An overview of the fundamentals of sequence stratigraphy and key definitions, *in* Wilgus, C.K., *et al.*, eds., Sea-level changes: an integrated approach, Society of Economic Paleontologists and Mineralogists, Special Publication no. 42, p. 39-45.

Zachos, J.C., Arthur, M.A., and Dean, W.E., 1989, Geochemical and paleoenvironmental variations across the Cretaceous/Tertiary boundary at Braggs, Alabama: Palaeogeography, Palaeoclimatology, Palaeoecology, v. 69, p. 245-266.

SOUTHEASTERN GEOLOGY
V. 34, No. 2, May 1994, p. 79-88

ANALYSIS OF OUTCROP-SCALE FAULT-RELATED FOLDS, EAGLE ROCK, VIRGINIA

S.A. KATTENHORN AND D.A. McCONNELL

Department of Geology
The University of Akron
Akron, OH 44325-4101

ABSTRACT

Geometric and kinematic models of fault-related folds predict a direct relationship between fault angle and fold shape and imply specific sequences of deformation. Analysis of outcrop-scale structures from Eagle Rock, Virginia, reveal fault-fold configurations that depart from model predictions.

A displacement-distance diagram is used to show that a thrust ramp loses displacement both up- and down-dip. The ramp is interpreted to have initiated at an intermediate nucleation point and propagated in both directions. Layers were initially folded ahead of the fault tips and were subsequently cut by the fault, producing both a hanging wall anticline and a footwall syncline.

Deformation styles are influenced by the character of the sedimentary rocks (rock types, relative thickness, order of units), an observation that is not readily incorporated into models of fault-fold interaction. A series of small displacement faults imbricated a competent sandstone unit where it lies between thicker, incompetent units (high ductility contrast). The incompetent unit responded with disharmonic folding and thickness changes above and below the fault ramps.

INTRODUCTION

Fault-bend folds (Figure 1a) are widely recognized in fold-and-thrust belts where thrust faults have a flat-ramp-flat geometry in stratigraphic sections with a well defined mechanical anisotropy (Boyer and Elliot, 1982; Kulander and Dean, 1986; Mitra, 1988). Fault-propagation folds (Figure 1b) form when a thrust ramp loses displacement upsection into a fold (Suppe, 1985; Chester and Chester, 1990; Suppe and Medwedeff, 1990). This fold style may be modified to create hybrid fault-bend folds if a ramp subsequently propagates parallel to layering to form an upper flat (Mitra, 1990). An implicit assumption of some fault-propagation fold models is that the thrust ramp propagated upsection from a lower detachment (Suppe and Medwedeff, 1984, 1990; Mitra, 1990). Eisenstadt and De Paor (1987) proposed an alternative hypothesis for ramp formation in which a thrust fault nucleates as a ramp in competent layers and propagates both upsection and downsection to link up with layer-parallel flats in incompetent units.

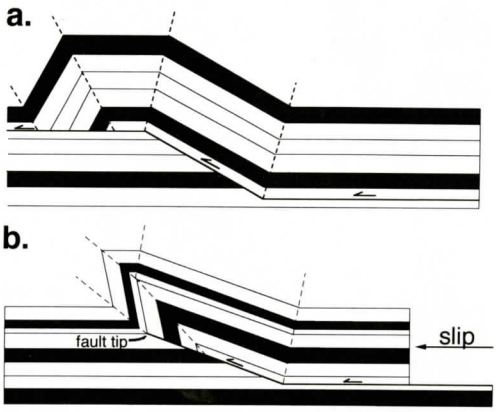

Figure 1.- a. Fault-bend fold. b. Fault-propagation fold (from Suppe, 1985).

Several geometric and kinematic models of fault-related folds have been developed in recent years as aids to structural interpretations in fold-and-thrust belts (Suppe and Medwedeff, 1984, 1990; Chester and Chester, 1990; Mitra, 1990). These models predict that fold geometry


a

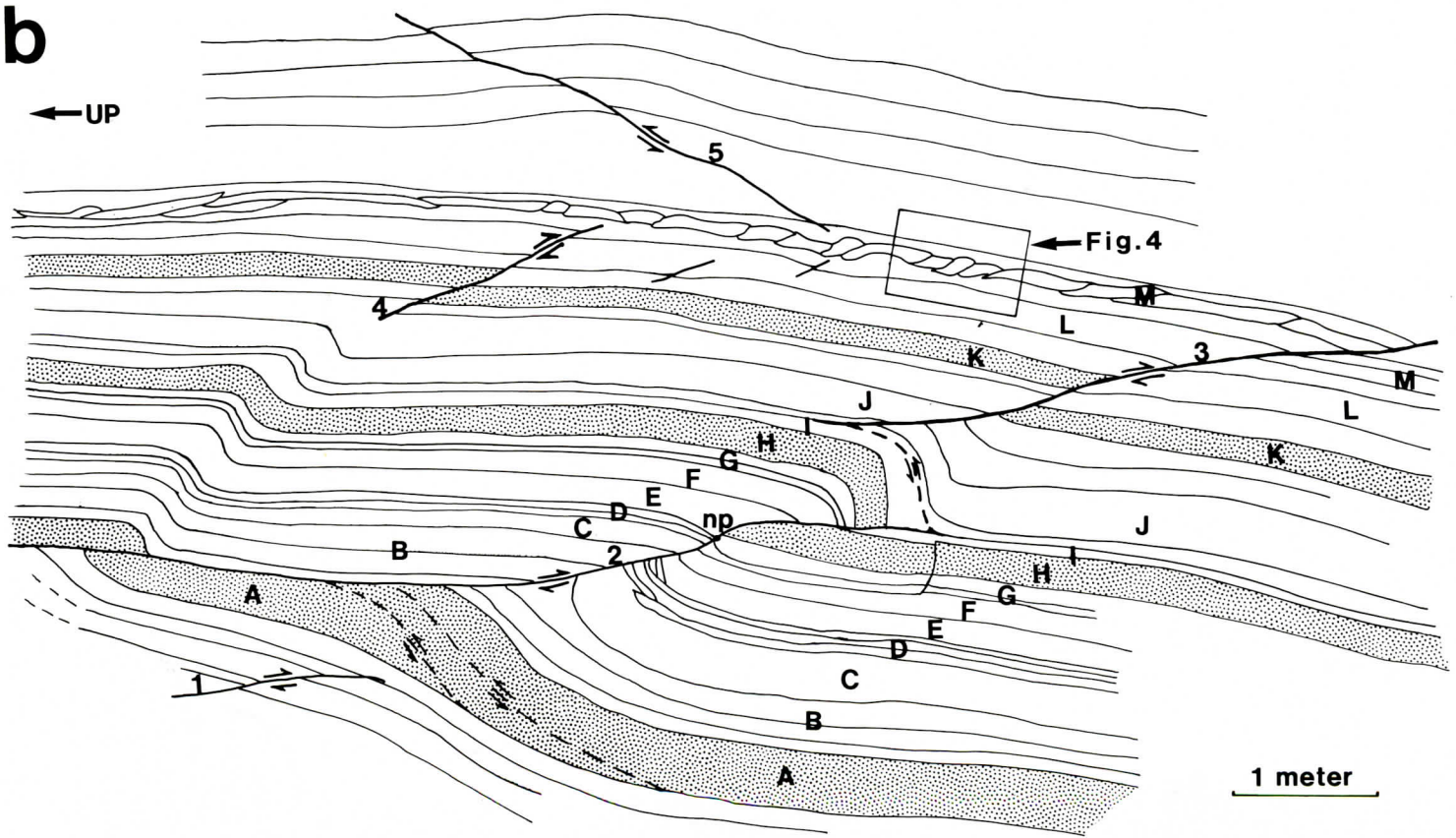

Figure 2.- a. Fault-related folding near Eagle Rock. Rocks are overturned, younger rocks to right. Note person for scale; b. Representation of 2a rotated to horizontal. Labeled beds and numbered faults are referred to in the text; np = nucleation point with respect to footwall, a matching point lies at the hanging wall cut-off of bed G. Area in box shown in Figure 4.

is dependent upon fault angle but do not address the influence of lithologic variations on fault propagation. An alternative procedure for the analysis of fault-fold relations involves consideration of the relative rates of fault slip and fault propagation (Williams and Chapman, 1983; McNaught and Mitra, 1993), factors controlled by the mechanical properties of the rock units. Muraoka and Kamata (1983) proposed that fault propagation was rapid relative to fault slip in competent layers, and considered incompetent units to be "strain absorbers" in which a fault would propagate slowly relative to displacement. The degree of folding and associated deformation must increase as the disparity between displacement and propagation rates increases (Chapman and Williams, 1984). Chester and others (1991) presented rock model experiments in which deformation style was influenced by the character of a mock stratigraphic interval (rock types, relative thickness and order of units). Their results suggested that deformation in thinly interbedded rock units is dependent upon the mean competence of the stratigraphic section rather than the competences of the individual layers.

Ellis and Dunlap (1988) documented examples of faults with local displacement maxima and minima along the fault plane. They interpreted the maxima to represent nucleation points for faults that subsequently propagated upsection and downsection, in accordance with the Eisenstadt and De Paor (1987) hypothesis.

Despite the existence of a hypothesis which predicts that thrust ramps propagate both upsection and downsection from competent beds (Eisenstadt and De Paor, 1987), observations that fault segments propagate both up- and down-dip (Ellis and Dunlap, 1988), and evidence that the mechanical properties of rock units influence folding (Muraoka and Kamata, 1983), there is a paucity of published examples of fault-fold relations that illustrate these features. This paper will describe an outcrop-scale fault-related fold that displays such characteristics. An associated imbricated, thin, sandstone layer enclosed within incompetent shales will also be described. Furthermore, the implications for interpretations of fault-related folds in thrust belts will be considered.

DESCRIPTION OF OUTCROP STRUCTURES

First-order fault-related folds in thrust belts typically involve a 1-2 km-thick section of sedimentary rocks (Fox, 1959; Perry, 1978; Boyer and Elliot, 1982; Kulander and Dean, 1986). The scale of these structures makes it impossible to view them in their entirety at the Earth's surface but many elements of their geometry are identifiable from well-log and seismic data (e.g. Mitra, 1988). However, the resolution of these data sets is rarely sufficient to define the details of fault-fold relations, and the cumulative deformation associated with thrust systems is often too complex to decipher the earliest stages of structural evolution. We describe a well-exposed, outcrop-scale fault-fold from the Valley and Ridge province of the Appalachian Mountains that can be described in its entirety and is free from overprinting of later deformation. In a study of deformation at thrust ramps in several outcrop-scale thrust faults, Serra (1977) attributed variable ramp styles to lithologic influences. This paper expands such analysis to include the nature of folding associated with the fault ramp.

Eagle Rock, Virginia

A series of fault-related folds occur in the Eagle Rock Gap road cut at the intersection of U.S. Highway 220 and State Highway 43, near Eagle Rock, Virginia. Regionally, the outcrop represents structures associated with the Pulaski-Staunton thrust sheet. A number of formations, ranging from Ordovician to Devonian age, are exposed in the cut (e.g. McGuire, 1970; Bartholomew and others, 1982). The structures described here occur in interbedded sandstones, siltstones and shales of the Silurian Rose Hill Formation; units of low to moderate ductility and a high ductility contrast. The

fault-related fold example is from the northwest end of the gap, where beds are overturned (Figure 2a). The road cut is a vertical face oriented perpendicular to strike and presents a cross-section view of fault-fold relations.

A line drawing of the outcrop is presented as Figure 2b; selected rock layers and faults are labelled by letter and number respectively. The most noticeable deformation occurred in the zone between faults 2 and 3 (Figure 2b), which are dip-slip faults that strike sub-parallel to bedding. Layers offset by fault 2 are folded and form both a hanging wall anticline and a footwall syncline (Figure 2b). The principal fault (2) cuts upsection on a 20° ramp (relative to bedding) from a flat above bed A, and becomes layer-parallel above bed I. Several beds in the footwall adjacent to the ramp are shortened by folding (B-G). Bed A lies in the footwall of the lower flat and is also folded; beds H and I are not folded in the footwall. The equivalent units in the hanging wall are offset on the ramp but only beds F-I exhibit significant folding. Beds J-L are offset by fault 3, which cuts upsection from above layer I at an 18° angle. Between faults 1 and 2, shortening is accommodated by backthrusting within bed A.

Displacement-distance diagrams may be constructed to illustrate the relationship between fault slip and fault length. The slope of the plotted line provides an indirect measure of deformation accommodated by factors other than fault displacement (e.g. folding; Chapman and Williams, 1984); steep lines are indicative of substantial folding and/or thickness changes whereas shallow slopes represent beds that have accommodated shortening without substantial folding (Chapman and Williams, 1984). Muraoka and Kamata (1983) classified displacement-distance curves as C-type (cone-shaped) or M-type (mesa-shaped). The C-type profiles are characteristic of incompetent rocks whereas the M-type profiles represent competent units that are surrounded by incompetent units (Muraoka and Kamata, 1983).

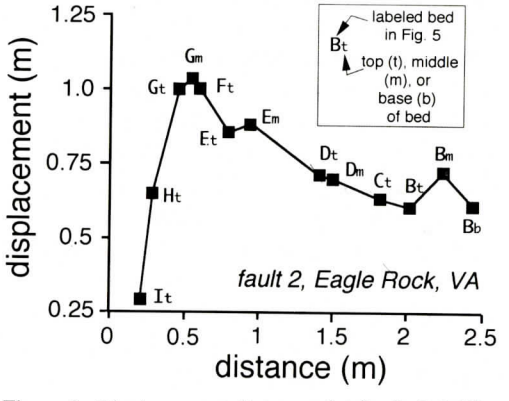

Figure 3.-Displacement-distance plot for fault 2 (Figure 2b) using a reference point at the top of the ramp. Approximate position of beds labeled in Figure 2b is shown.

Displacement along fault 2 decreases upsection and downsection from a maximum at point np (Figures 2b,3). The resultant profile (Figure 3) conforms to the C-type of Muraoka and Kamata (1983). Small variations in the profile are interpreted to be the result of lithologic effects (e.g. bed thickening in shale). The relative smoothness of the profile is interpreted to indicate essentially uniform relative rates of fault displacement and fault propagation through the lithologic section. This interpretation is supported by Chester and others' (1991) simulations of faulting in interbedded competent and incompetent units which acted as a single structural lithic unit with a high mean ductility.

The position of the upper tip of the fault was estimated (from Figure 3) by projecting the steeply inclined segment of the plot down to the distance axis. The intersection point corresponds to a position in a thin shale layer on the hanging wall flat approximately 0.2 meters to the right of the top of the ramp (Figures 2b,3). This suggests that fault 2 did not propagate far on the upper flat. Fault 3 flattens downward into the same shale layer, and faults 2 and 3 are interpreted to be linked by a layer-parallel detachment in the shale layer (between I and J, Figure 2b). This allows a complex interplay between the displacements along faults 2 and 3, similar to that observed in triangle zones along the frontal segments of fold and thrust belts (e.g. Banks and Warburton,

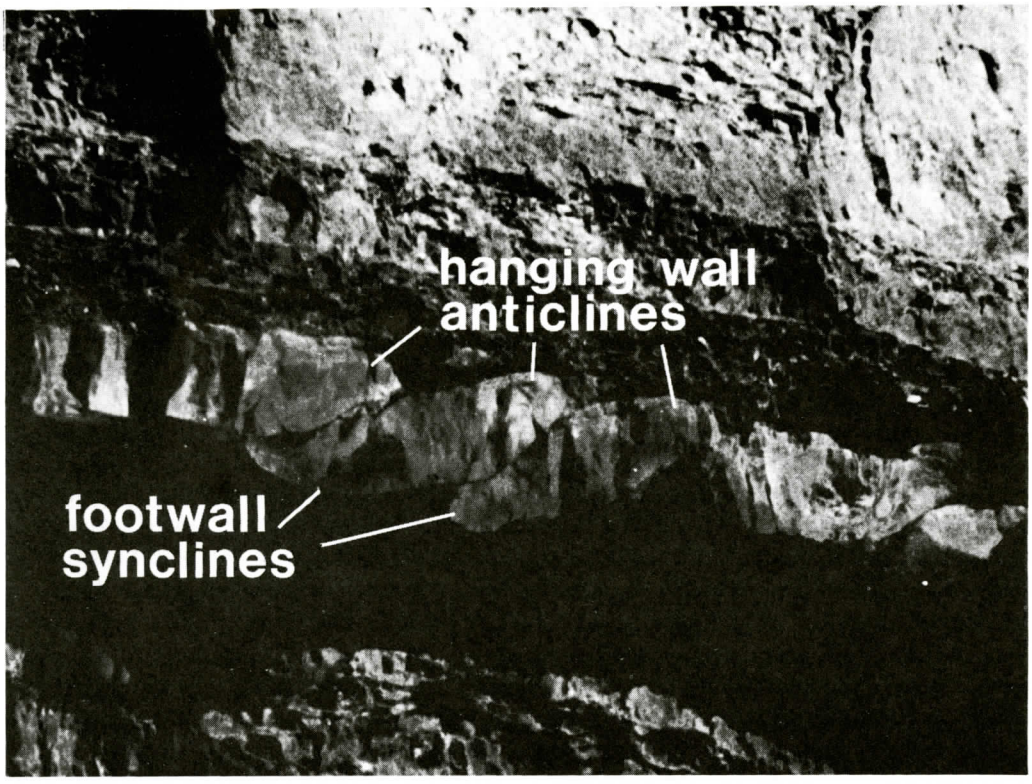

Figure 4.-Oblique-view of rotated fault blocks in imbricated sandstone bed (8 cm thick). Location of this figure shown on Figure 2b.

1986). There is a consistent amount of shortening on faults 2 and 3. Measurements of shortening of beds above (J) and below (H) the proposed detachment horizon yield similar values (9% and 12% respectively). We interpret this to indicate that faults 2 and 3 propagated independently, with later linkage along the layer-parallel detachment.

A contrasting deformation style is observed locally in a thin (8cm) sandstone layer (bed M, Figures 2b,4) sandwiched between thicker shale layers. The sandstone bed is imbricated by more than 20 faults which typically (but not exclusively) have the same sense of displacement as faults 2 and 3. The surrounding shales contain disharmonic folds, or exhibit thickness changes, above and below the fault ramp. We interpret this to indicate that fault displacement was accommodated by folds in the shale.

The imbrication of a layer by several thrust faults typically leads to the formation of a duplex or imbricate fan distinguished by the presence (duplex) or absence (imbricate fan) of a roof thrust (Boyer and Elliott, 1982). In both cases the thrust faults are assumed to ramp upsection from a planar floor thrust (Boyer and Elliott, 1982). The geometry of the resultant structures is determined by ramp spacing and the amount of displacement on each fault (Mitra and Boyer, 1986; Tanner, 1992). Gretener (1972) recognized that a series of independent ramp anticlines are generated where fault displacement is significantly less than the spacing between adjacent ramps (see also Mitra, 1986). Displacement on faults in bed M is small relative to the distance between ramps (Figures 2b,4). Small ramp anticlines can be identified above each ramp, as expected for fault-bend folding, however, ramp synclines are also present (Figure 4) and these structures are not represented in descriptions of

either imbricate fans or duplexes. Extensional fractures that are oriented parallel to the fold axes and normal to layering are observable on the outer (lower) surface of some of the footwall synclines.

DISCUSSION

Fault-bend and fault-propagation fold models (Rich, 1934; Suppe, 1985; Jamison, 1987; Suppe and Medwedeff, 1990; Mitra, 1990) typically assume: 1. footwall rocks are undeformed (for exceptions, see Ramsay, 1992; McNaught and Mitra, 1993); 2. initial slip occurs on a layer-parallel detachment plane; and, 3. displacement is either constant (fault-bend folds) or decreases uniformly upsection (fault-propagation folds) (Figure 1).

Deformation styles recognized at Eagle Rock do not match those featured in geometric and kinematic models as: 1. the thrust ramp loses displacement both up-dip and down-dip; 2. ramps may not join a lower and/or upper detachment (flat); 3. footwall rocks may be folded to form synclines.

The loss of displacement both up- and downsection from a point near the center of the fault (Figures 2b,3) is interpreted to indicate that the fault nucleated in a competent sandstone bed and propagated both updip and downdip. Unfaulted layers initially accommodated shortening by folding ahead of the propagating fault tip. The folds were subsequently cut by the fault (Figure 5) which became layer parallel at the tops of beds A and I. Consequences of this deformation sequence are that both footwall and hanging wall rocks are folded, and displacement decreases along the fault from the nucleation point toward the fault tips.

The principal fault-related fold pair at Eagle Rock is essentially symmetrical about the fault plane (fault 2), presumably because the stratigraphic section is relatively uniform both above and below the nucleation point (competent sandstones with interbedded shales and siltstones). In contrast, a duplex-like structure is formed in a thin sandstone layer (bed M, Figure 4) between shale layers of greater thickness, a section of moderate mean ductility and high ductility contrast (Donath and Parker, 1964). Shortening of this layer occurred as a result of slip on a series of small-displacement faults rather than by displacement on a single fault plane.

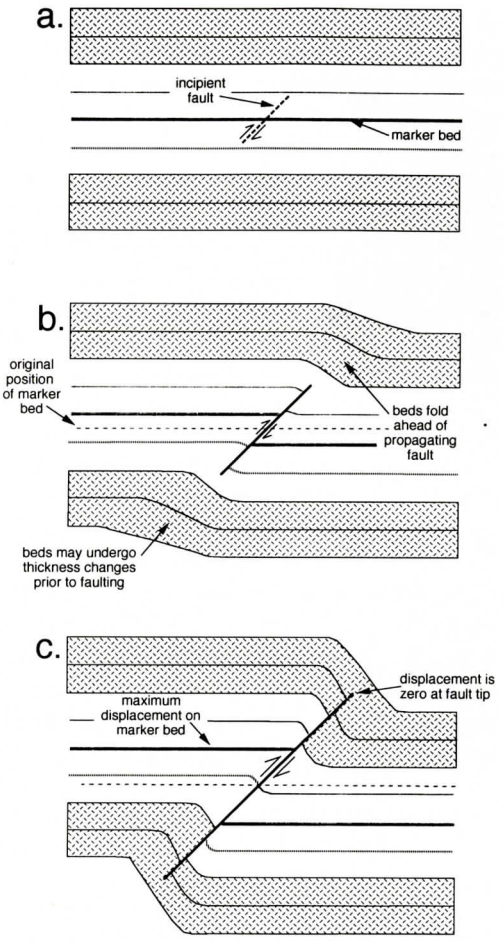

Figure 5.-Sequence of folding and faulting above and below a propagating fault. a. configuration prior to slip on the fault; b. initial fault slip and propagation results in displacement of marker bed and symmetrical folding of units above and below fault tips; c. continued fault propagation increases fault length. Displacement decreases from a maximum represented by offset marker bed to a minimum of zero at fault tips.

The apparent symmetry between the form

of the folds at the top and the bottom of the fault 2 ramp, and adjacent to ramps in bed M, is interpreted to indicate an analogous fold evolution. Ramp anticlines form when hanging wall rocks are distorted as they pass from a ramp onto an upper flat (Boyer and Elliott, 1982; Mitra, 1986). We interpret the footwall synclines to have been generated as footwall rocks were displaced from the ramp onto a lower flat. This mechanism entails that both hanging wall and footwall rocks were displaced relative to an original datum (Figure 5; Williams and Chapman, 1983) in contrast with conventional interpretations in which the hanging wall is displaced and the footwall rocks remain fixed. We do not discount the possibility that some limited folding may predate faulting (e.g. break-thrust folds; Fischer and others, 1992), however, fold amplitude increases with decreasing displacement, therefore, most of the folding is interpreted to have been coeval with faulting. The common view of thrust faults cutting upsection from a basal detachment plane leads to the assumption that only hanging wall rocks are deformed. In contrast, the analyses of Eisenstadt and De Paor (1987) and Williams and Chapman (1983) require that deformation occurs in both the hanging wall and footwall as a fault propagates updip and downdip from a nucleation point.

Fault-bend folds may accommodate hanging wall deformation by slip on layer-parallel hanging-wall flats (Figure 1a), slip on antithetic thrust faults (Banks and Warburton, 1986; Geiser, 1988), or by folding and/or cleavage development (Geiser, 1988; Ferrill and Dunne, 1989). These mechanisms remove the kinematic necessity for a roof thrust and the faults may then be viewed as an imbricate fan or an autochthonous roof duplex (Geiser, 1988). However, if faults lose displacement both up- and down-dip into adjacent deformation to produce a duplex-like structure that lacks the typical features of duplexes, such as roof and floor thrusts (Figure 6), then neither term is appropriate.

Current models of fault-related folds (e.g. Mitra, 1990; Suppe and Medwedeff, 1990)

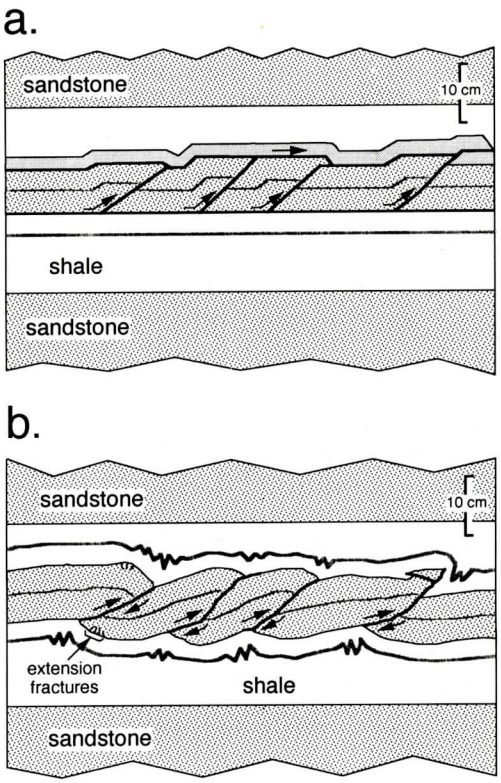

Figure 6.-Fault imbrication of a layer by; a. a duplex; b. thrust faults without associated hanging wall and footwall flats, shortening in adjacent shale layers accommodated by disharmonic folding. Fault blocks are surrounded by faults in (a) but are only bounded by faults at ramps in (b).

incorporate faults that propagate upwards from a basal detachment plane and such deformation styles are well documented (Boyer and Elliott, 1982; Kulander and Dean, 1986; Mitra, 1988) where a thick section of competent rocks overlies a relatively thin detachment zone (e.g. lower Paleozoic section in central Appalachians). Cross sections through fold-and-thrust belts have rarely illustrated faults that lose displacement both up- and downsection (for an exception see Fox, 1959), but this deformation style may be more prevalent where competent units are surrounded by moderate-high ductility rocks (e.g. Mesozoic rocks, Canadian Rocky Mountains, Fox, 1959; middle Ordovician-Devonian section, central Appalachians,

Mitra, 1988).

Natural first-order thrust faults contain footwall structures (Protzman and Mitra, 1990; Evans and Neves, 1992; McNaught and Mitra, 1993) that are not predicted by classic fault-related fold models. Such deformation cannot be readily accounted for by many of the geometric and kinematic models constructed to simulate fold-fold interactions. An interpretation governed by the mechanical response of the faulted units may be more appropriate when endeavoring to explain anomalous deformation styles and requires greater understanding of fault-fold relations in multilithologic stratigraphic sections.

SUMMARY

These natural faulted folds exhibit several characteristics that are interpreted to support the hypotheses forwarded by Eisenstadt and De Paor (1987) that thrust faults initiate as ramps and propagate both up-dip and down-dip. This is confirmed using a displacement-distance graph and interprets a displacement maximum as the location of a fault nucleation point. Displacement decreases up-dip and down-dip as the fault propagated away from the nucleation point and lost displacement into folds. Shortening may be accommodated by different mechanisms in competent and incompetent rocks and this may result in the formation of duplex-like structures of rotated fault blocks that lack floor and roof thrusts.

ACKNOWLEDGMENTS

Reviews and comments by Gautam Mitra and Kevin Stewart helped improve on the original version of this manuscript. Simon Kattenhorn acknowledges research grants from the American Association of Petroleum Geologists and Sigma Xi.

REFERENCES

Banks, C.J., and Warburton, J., 1986, `Passive-roof' duplex geometry in the frontal structures of the Kirthar and Sulaiman Mountain belts, Pakistan: Journal of Structural Geology, v. 8, p. 229-237.

Bartholomew, M.J., Schultz, A.P., Henika, W.S., and Gathright, T.M., II, 1982, Geology of the Blue Ridge and Valley and Ridge at the junction of the central and southern Appalachians: *in* Lyttle, P.T., ed., Central Appalachian Geology, NE-SE Geological Society of America, Field Trip Guidebooks, p. 121-170.

Boyer, S.E., and Elliott, D., 1982, Thrust systems: American Association of Petroleum Geologists Bulletin, v. 66, p. 1196-1230.

Chapman, T.J., and Williams, G.D. 1984, Displacement-distance methods in the analysis of fold-thrust structures and linked fault systems: Journal of the Geological Society of London, v. 141, p. 121-128.

Chester, J., and Chester, F. 1990, Fault propagation folds above thrusts with constant dip: Journal of Structural Geology, v. 12, p. 903-910.

Chester, J.S., Logan, J.M., and Spang, J.H., 1991, Influence of layering and boundary conditions on fault-bend and fault-propagation folding: Geological Society of America Bulletin, v. 3, p. 1059-1072.

Donath, F.A., and Parker, R.B., 1964, Folds and folding: Geological Society of America Bulletin, v. 75, p. 45-62.

Eisenstadt, G., and De Paor, D.G. 1987, Alternative model of thrust-fault propagation: Geology, v. 15, p. 630-633.

Ellis, M.A., and Dunlap, W.J., 1988, Displacement variation along thrust faults: implications for the development of large faults: Journal of Structural Geology, v. 10, p. 183-192.

Evans, J.P., and Neves, D.S., 1992, Footwall deformation along Willard thrust, Sevier orogenic belt: implications for mechanisms, timing, and kinematics. Geological Society of America Bulletin, v. 104, p. 516-527.

Ferrill, D.A. and Dunne, W.M., 1989, Cover deformation above a blind duplex: an example from West Virginia, U.S.A.: Journal of Structural Geology, v. 11, p. 421-431.

Fischer, M.P., Woodward, N.B., and Mitchell, M.M., 1992, The kinematics of break-thrust folds: Journal of Structural Geology, v. 14, p. 451-460.

Fox, F.G., 1959, Structure and accumulation of hydrocarbon in Southern Foothills, Alberta, Can-

ada: American Association of Petroleum Geologists Bulletin, v. 43, p. 992-1025.

Geiser, P.A., 1988, Mechanisms of thrust propagation: some examples and implications for the analysis of overthrust terranes: Journal of Structural Geology, v. 10, p. 829-845.

Jamison, W.R. 1987. Geometric analysis of fold development in overthrust terranes: Journal of Structural Geology, v. 9, p. 207-219.

Kulander, B.R., and Dean, S.L., 1986, Structure and tectonics of central and southern Appalachian Valley and Ridge and Plateau Provinces, West Virginia and Virginia: American Association of Petroleum Geologists Bulletin, v. 70, p. 1674-1684.

McGuire, O.S., 1970, Geology of the Eagle Rock, Strom, Oriskany, and Salisburg quadrangles, Virginia: Virginia Division of Mineral Resources Report of Investigations, v. 24, 39p.

McNaught, M.A., and Mitra, G., 1993, A kinematic model for the origin of footwall synclines: Journal of Structural Geology, v. 15, p. 805-808.

Mitra, S., 1986, Duplex structures and imbricate thrust systems: geometry, structural position and hydrocarbon potential: American Association of Petroleum Geologists Bulletin, v. 70, p. 1087-1112.

Mitra, S., 1988, Three-dimensional geometry and kinematic evolution of the Pine Mountain thrust system, Southern Appalachians: Geological Society of America Bulletin, v. 100, p. 72-95.

Mitra, S. 1990, Fault-propagation folds: Geometry, kinematic evolution, and hydrocarbon traps: American Association of Petroleum Geologists Bulletin, v. 74, p. 921-945.

Mitra, G., and Boyer, S.E., 1986, Energy balance and deformation mechanisms of duplexes: Journal of Structural Geology, v. 8, p. 291-304.

Muraoka, H., and Kamata, H., 1983, Displacement distribution along minor fault traces: Journal of Structural Geology, v. 5, p. 483-495.

Perry, W.J., Jr., 1978, Sequential deformation in the central Appalachians: American Journal of Science, v. 278, p. 518-542.

Protzman, G.M., and Mitra, G., 1990, Strain fabric associated with the Meade thrust sheet: implications for cross-section balancing: Journal of Structural Geology, v. 12, p. 403-417.

Ramsay, J.G., 1992, Some geometric problems of ramp-flat thrust models: *in* McClay, K.R., ed., Thrust tectonics, Chapman-Hall, London, p. 191-200.

Rich, J.L., 1934, Mechanics of low-angle overthrust faulting as illustrated by Cumberland thrust block, Virginia, Kentucky and Tennessee: American Association of Petroleum Geologists Bulletin, v. 33, p. 1643-1654.

Serra, S., 1977, Styles of deformation in the ramp regions of overthrust faults: Wyoming Geological Association, Annual Field Conference, 29th, Guidebook, p. 487-498.

Suppe, J., 1985, Principles of structural geology. Englewood Cliffs, New Jersey, Prentice-Hall, 537p.

Suppe, J., and Medwedeff, D.A., 1984, Fault-propagation folding: Geological Society of America Abstracts with Programs, v. 16, p. 670.

Suppe, J., and Medwedeff, D.A., 1990, Geometry and kinematics of fault-propagation folding: Eclogae geologicae Helvetiae, v. 83, p.409-454.

Tanner, P.W.G., 1992, Morphology and geometry of duplexes formed during flexural-slip folding: Journal of Structural Geology, v. 14, p. 1173-1192.

Williams, G.D. & Chapman, T.J. 1983, Strains developed in the hanging walls of thrusts due to their slip/propagation rate: a dislocation model: Journal of Structural Geology, v.6, p.563-571.

SOUTHEASTERN GEOLOGY
V. 34, No. 2, May 1994, p. 89-97

PLEISTOCENE MOLLUSCAN FAUNAS FROM CENTRAL MISSISSIPPI VALLEY LOESS SITES IN ARKANSAS, TENNESSEE, AND SOUTHERN ILLINOIS

BARRY B. MILLER
Department of Geology
Kent State University
Kent OH 44242

JUNE E. MIRECKI
Department of Geological sciences
Memphis State University
Memphis, TN 38152

LEON R. FOLLMER
Illinois State Geological Survey
Champaign IL 61820

ABSTRACT

Fossil gastropods have been identified in Wisconsinan (Peoria and Roxana silt) units exposed in the Wittsburg Quarry area of Crowleys Ridge, Arkansas. Previous reports of molluscs from this area have been limited to those recovered from a third loess (=? Loveland/Sicily Island loess). Nine species have been identified from the Peoria Loess, 13 from the Roxana Silt and 19 from the third loess (Loveland correlative). Each of these units include taxa that now reach the southern limits of their geographic range in the Mississippi Valley well upstream from the fossil site at Wittsburg. Extralimital species include *Allogona profunda*, *Vertigo gouldi*, *V. tridentata*, and *Zontitoides limatulus*, in the third loess; and *Hendersonia occulta*, and *Nesovitrea electrina*, in all three units. Although none of these species are truly boreal in their modern distributions, they all probably required cooler summer temperatures to permit southward range extensions during the times of eolian silt deposition. Similarity of molluscan faunas from the Wittsburg Quarry suggest that analogous environmental conditions existed at the time the three silt units accumulated.

Comparison of the Wittsburg Quarry molluscs with fossils recovered from central Mississippi Valley deposits exposed upstream in Tipton County, Tennessee and Powdermill Creek, in St. Clair County, Illinois, reveal a general decrease in the boreal-arctic faunal elements commonly found in the Illinoian and Wisconsinan loess faunas to the north of Crowleys Ridge.

INTRODUCTION

Rarely are several cycles of fossiliferous Wisconsinan and pre-Wisconsinan loess deposits found in superposition in situations that permit the use of independent dating methods to provide chronostratigraphic control. Recent studies in the Wittsburg Quarry area of Crowleys Ridge (Figure 1) have identified the presence of gastropods in the Peoria and Roxana silt units (Mirecki and Miller, 1994). Previous reports of molluscs from this area have been limited to those recovered for amino acid studies from a third loess (Figure 2) exposed below the Roxana Silt at the Crowleys Ridge, Arkansas (Mirecki and Miller, 1994; Clark and others 1989). Clark and others (1989) used the name Loveland for the third loess at Wittsburg Quarry, which they correlated with the Illinoian Loveland Loess of western Iowa and Chinatown silt of southwestern Illinois, on the basis of stratigraphic position and amino acid epimerization values from snail-shell protein.

Autin and others (1991), however, corre-

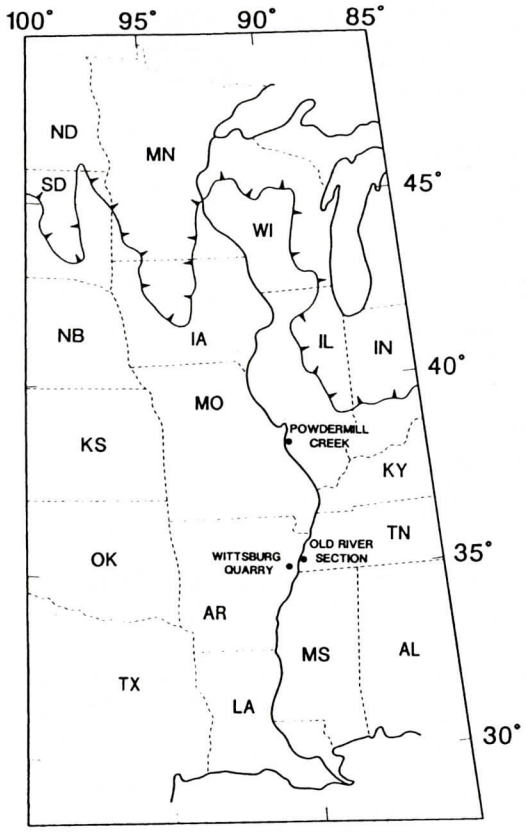

Figure 1. Map showing location of Wittsburg Quarry, Old River section and Powdermill Creek.

late the third loess with the Sicily Island Loess of Louisiana, which they consider early Wisconsinan on the basis of stratigraphic position and geosol development. To avoid this controversy of nomenclature we use the term third loess. Amino acid data presented in Mirecki and Miller (1994) support an Illinoian age interpretation for the third loess.

The Wittsburg Quarry sequence provides an unusual opportunity to study faunal and environmental conditions at a single geographic location through at least three eolian cycles. The relative age interpretations of these deposits are based on amino acid epimerization (aIle/Ile) values from terrestrial gastropods, which have been used to define and identify three aminozones that correlate with the Peoria Loess, Roxana Silt, and third loess (Mirecki and Miller, 1994). The amino acid epimerization values for the aminozone based on shells recovered from the Roxana Silt have been calibrated with two radiocarbon age estimates obtained at the Wittsburg Quarry (Figure 2). A minimum age estimate for the Peoria Loess aminozone was provided by a radiocarbon date on carbon at Old River section (Figure 2).

In this study we provide environmental interpretations and comparisons of the molluscan fossils from the Peoria, Roxana and third loess sediments at the Wittsburg Quarry, and from two other central Mississippi Valley sites upstream from Wittsburg Quarry. The Peoria Loess exposed at the Old River section, in Tipton County, Tennessee, includes molluscs that occur approximately 1 m above the sample collected for the radiocarbon age estimate from the Roxana Silt.

The second collection of molluscs is from Illinoian sediments (Chinatown silt) exposed at Powdermill Creek, in St. Clair County, Illinois, east of St. Louis (Clark and others 1989). Although the age relationship between the Chinatown silt in the Powdermill Creek area and the third loess at Wittsburg Quarry is not yet clear, the correlation between these units suggested in Clark and others (1989) is tentatively accepted. At several localities in the Powdermill Creek area, however, the Chinatown silt occurs stratigraphically below younger Illinoian units, the Fort Russell till and Teneriffe Silt (McKay, 1989). Therefore, although the molluscs from the Chinatown silt are Illinoian, they may not be isochronous with the third loess molluscs from Wittsburg Quarry. The Powdermill Creek molluscs are included because they may represent the nearest Mississippi Valley Illinoian age locality with molluscs for which there are available amino acid epimerization data for comparison with the third loess at Wittsburg Quarry.

MOLLUCAN FAUNAL ANALYSIS

Collection Methods

The fossils reported here are from collec-

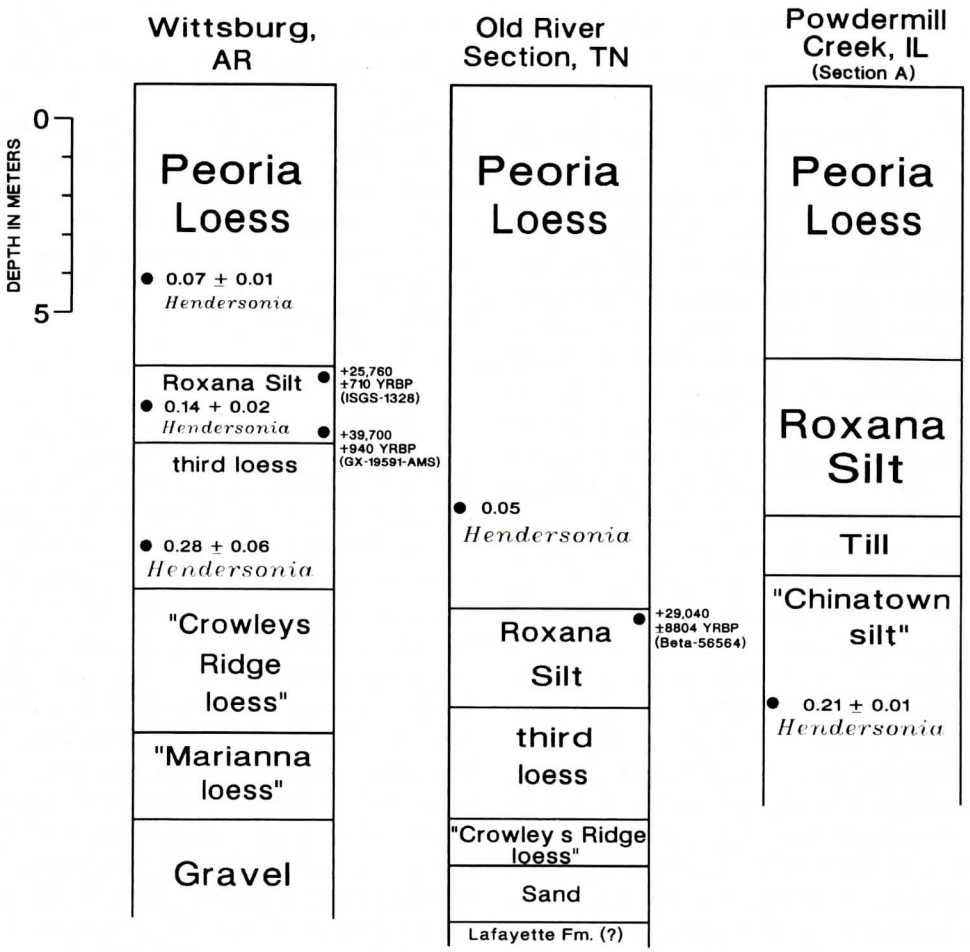

Figure 2. The mean total acid hydrolysate values for *Hendersonia* from Memphis State Geochronology Laboratory and radiocarbon ages superimposed on the stratigraphy at Wittsburg Quarry, Old River section and section A at Powdermill Creek. (Modified from Clark and others, 1989).

tions made between 1984 and 1992, by different workers, using different collecting methods, and that usually were made for purposes other than study of the molluscan paleontology of the deposits. No standard collecting methods were used. The collections made earlier from the third loess at Wittsburg Quarry and Powdermill Creek by Donald McKay, Illinois State Geological Survey, included small bulk samples and shells picked from surface exposures. Subsequently, bulk samples of ca. 30 kg and 50 kg, respectively, were made from the third loess at Wittsburg Quarry and Chinatown silt at section A, Powdermill Creek. In addition, a small sample of ca. 2 kg was recovered from secton B at Powdermill Creek. Faunal analysis of shell, screen-washed from these samples, include most of the taxa present in the surface exposures, as well as some species not represented in the small bulk samples or surface collections. Smaller bulk collections of approximately 15 kg each were made from the Peoria and Roxana loesses at Wittsburg Quarry and Peoria Loess at Old River section, for the purpose of recovering shells for amino acid studies.

In spite of limitations imposed by the collecting methods, much useful information about local environmental conditions extant during the time the fossil lived can be inferred

from the fossils recovered from these sites.

Wittsburg Quarry

The Wittsburg Quarry is located in the NE 1/4, Sec. 32, T. 7 N., R. 4 E., Cross County, Arkansas (Wittsburg 7.5′ quadrangle). Seven hundred sixteen individuals representing 26 species of gastropods, four of which are represented by a single individual, have been identified from the three stratigraphic units at Wittsburg Quarry (Table 1). Species diversity and individual abundance counts from each stratigraphic unit appear to primarily reflect the quantity of matrix processed to recover the fossils (Table 1). All of the Wittsburg molluscan taxa are extant and belong to taxa that now are limited to terrestrial habitats. The lack of aquatic species imply the absence of water bodies near the deposition site. Five terrestrial species, *Gastrocopta contracta, G. holzingeri, Hawaiia minuscula, Helicodiscus parallelus* and *Strobilops labyrinthica*, comprise more than 50% of the individuals in each of the three fossiliferous loess units at Wittsburg Quarry. In addition, *Gastrocopta armifera, Hendersonia occulta* and *Nesovitrea electrina* also occur in all three silt units. These eight species occur in association with large woodland taxa such as *Triodopsis fosteri, Anguispira alternata* and *Allogona profunda* in the third loss, suggesting the presence of a well-drained forest of oak, hickory, elm and ironwood near the deposition site.

The larger species appear to be represented in the younger silt units at the Wittsburg Quarry by shell fragments that cannot be identified satisfactorily to genus or species. The dissimilarity that exist between the faunas of third loess and younger loess units at Wittsburg Quarry can be ascribed to differences in preservation and sample size and have no environmental significance. The molluscan faunas from the three units appear to have lived under similar environmental conditions.

Distribution maps in Hubricht (1985) indicate that each of the fossiliferous silt units include taxa that now reach the southern limits of their geographic range in the Mississippi Valley well upstream from the fossil site at Wittsburg. The extralimital species include *A. profunda, Vertigo gouldi, V. tridentata,* and *Zontitoides limatulus*, in the third loess; and *H. occulta,* and *N. electrina*, in all three units. Although none of these species are truly boreal in their modern distributions, they all probably required cooler summer temperatures to permit southward range extensions during the times of eolian silt deposition.

Old River Section

The Old River section is a bluff exposure 200 feet southeast of Herring Hill Road, 1-3/4 miles west southwest of Dixonville, Tennessee (lat 35°25'04" N; long 89°58'29" W), Drummonds 7.5' quadrangle. The section is described in Parks and Lounsbury (1975). The Peoria Loess sample from here includes 420 individuals representing 23 species, three of which are represented by single individuals (Table 1). Seventy percent of the individuals in the Peoria Loess at this site are represented by five species, *Pomatiopsis lapidaria, Hendersonia occulta, Strobilops labyrinthica, Hawaiia minuscula,* and *Helicodiscus parallelus*. The assemblage is dominated by *P. lapidaria*, an amphibious rather than truly aquatic snail that can usually can be found living on moist soil near water; on plant litter kept moist by groundwater seepage; or climbing on the lower portions of cattail (*Typha*) or bulrush (*Scirpus*) (Clarke, 1981; Dundee, 1957; Jokinen, 1992).

The presence at the Old River section of *P. lapidaria* and *Carychium exile*, two species that live in or near water, suggests the presence of spring seepage that provided moist to wet habitats near the deposition site. There are, however, no truly obligate aquatic taxa in the Old River section assemblage, and consequently there is no evidence for either permanent or temporary water bodies near the deposition site.

Powdermill Creek Section

An Illinoian age for the Chinatown silt at Powdermill Creek is based on its stratigraphic position beneath the Fort Russell till (Figure 3).

Table 1. Abundance distribution and habitat preference of molluscs from Wittsburg Quarry, Old River section and Powdermill Creek. 1= Quiet water bodies which may fluctuate in depth seasonally; 2= Swamps, marginal habitats with sedges and other plants near waters edge: 3= Wooded areas with moist leaf mold and forest litter; usually close to water on floodplain: 4=Wooded areas; ground moisture related to season: 5=Scattered trees, grass, shrubs; well drained valley slopes with limestone bluffs; species do not require forests: 6=Open area with grass, shrub cover; species are dought resistant.

	WITTSBURG QUARRY			OLD RIVER SECTION	POWDER-MILL CREEK	HABITAT
TAXON	Peoria Loess ~15 kg*	Roxana Silt ~15 kg	Third Loess ~30 kg	Peoria Loess ~15 kg	Chinatown Silt ~50 kg	
Allogona profunda	--	--	9	4	--	2,3,4
Anguispira alternata	--	--	10	10	12	3,4,5
Aplexa hypnorum	--	--	--	--	2	1
Carychium exile	--	--	--	8	22	2,3
Catinella sp.	--	4	--	4	19	?
Cionella lubrica	--	1	--	12	1	3
Columella sp.	--	--	1	--	2	?
Deroceras aenigma	--	--	--	--	4	?
Discus cronkhitei	--	--	--	15	1	3
Discus macclintocki	--	--	--	--	4	3
Discus patulus	--	--	--	2	--	3,4
Euconulus fulvus	--	1	--	1	14	3,4
Fossaria exigua	--	--	--	--	17	1
Gastrocopta armifera	5	18	39	--	4	3,4,5,6
Gastrocopta contracta	12	33	33	10	1	2,3,4,5
Gastrocopta corticaria	--	--	1	--	--	2,3,4
Gastrocopta holzingeri	18	46	3	--	--	2,3,4,5
Gastrocopta pentadon	--	--	18	10	3	4,5,6
Haplotrema concavum	--	--	3	1	3	3,4,5
Hawaiia minuscula	10	27	17	27	13	3,4,5,6
Helicodiscus parallelus	14	18	68	17	22	3,4,5
Hendersonia occulta	7	9	52	24	7	3,4
Mesomphix friabilis	--	3	2	--	--	2
Nesovitrea electrina	2	5	18	--	18	2,3,4
Pisidium casertanum	--	--	--	--	1	1
Pisidium ventricosum	--	--	--	--	1	1
Planorbula armigera	--	--	--	--	1	1
Pomatiopsis lapidaria	--	--	--	206	21	2
Punctum minutissimum	--	2	22	14	44	3,4
Retinella indentata	--	--	--	10	--	3,4,5
Stenotrema hirsutum	1	--	4	--	29	3,4,5
Stenotrema leai	--	5	--	--	--	2,3,4,5
Striatura milium	--	--	--	1	25	4,5
Strobilops labyrinthica	39	33	78	24	36	3
Succinea ovalis	--	--	--	--	4	3,4
Triodopsis albolabris	--	--	--	3	--	3
Triodopsis fosteri	--	--	3	3	--	5
Triodopsis multilineata	--	--	--	--	1	2,3
Vallonia cf. *gracilicosta*	--	--	--	--	2	3,4,5
Vallonia parvula	--	2	--	--	--	3,4,5
Vallonia sp.	2	--	--	--	--	?
Vertigo elatior	--	--	--	2	31	3
Vertigo gouldi	--	--	1	--	--	2?
Vertigo milium	--	4	--	--	1	2
Vertigo nylanderi	--	--	--	--	1	2?
Vertigo tridentata	--	--	5	--	--	4,5
Zonitoides arboreas	3	--	2	12	7	3,4,5
Zonitoides limatulus	--	--	3	2	--	3,4
TOTALS	113	211	392	420	374	

* Approximate weight of sample processed for molluscs.

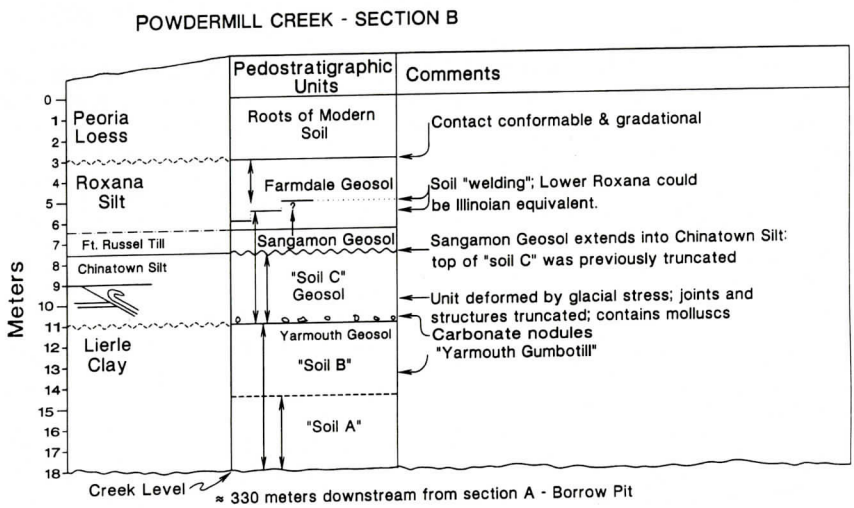

Figure 3. Stratigraphy at Powdermill Creek, section B.

At the reference section for the Chinatown silt, near Marysville, 21 km (13 mi) north of Powdermill Creek, the degree of weathering in the Chinatown silt suggests an interglacial geosol (McKay, 1989). Although the solum of this geosol is missing at Powdermill Creek, the Chinatown silt at this locality is bounded by what are interpreted as the Sangamon and Yarmouth Geosols, and therefore is considered Illinoian in age.

The molluscs from the Chinatown silt are from collections made at a borrow pit developed in a bluff just to the southeast of Powdermill Creek, in NW1/4 NE1/4 NW1/4 Sec. 10, T.1 N., R. 9 W., and from exposures along Powdermill Creek, about 330 m downstream in NE1/4 NW1/4 NW1/4 St. Clair County, Ilinois, French Village 7.5′ quadrangle (Figures 2 and 3). The larger shell collection is from silt exposed near base of the borrow pit. Shell from this collection yielded the original amino acid epimerization data reported in Clark and others (1989, p. 922). Correlation between collection sites at Powdermill Creek is based on physical tracing of the stratigraphic units exposed at the borrow pit (section A) to the cutbank exposure (section B), (Figure 3); and from the similar amino acid epimerization values obtained for the same taxa from each collection site (Table 4). The similarity of the physical stratigraphy and amino acid epimerization values appears to justify treating all of the fossils collected from the Chinatown silt as a single assemblage. A molluscan fauna of 31 species of gastropods and clams, identified from shell collections of 374 individuals. Nine of the species, however, are only represented by single individuals (Table 1). The presence of some type of aquatic habitat is implied by the occurrence of the amphibious species *Pomatiopsis lapidaria*, associated with such obligate aquatic taxa as *Pisidium* spp., *Planorbula armigera, Aplexa hypnorum* and *Fossaria exigua*. This inference is further supported by the presence of several terrestrial taxa, *Succinea ovalis, Vertigo elatior* and *Carychium exile*, which prefer damp places near water (Burch and Jung, 1988). The presence of *Aplexa hypnorum*, a snail that is usually associated with ephemeral ponds, implies that the water was subject to significant seasonal drying.

If we accept the possibility that the one individual identified as *Vertigo nylanderi* may be reworked, there still remain three terrestrial species, *V. elatior, H. occulta*, and *Discus macclintocki* in the Powdermill Creek assemblage that are no longer living in the St. Clair County area of Illinois (Baker, 1939). *Vertigo elatior* has been reported from Rockford County, Illinois (Baker, 1939) and both *H. occulta* and *D.*

Table 2. Faunal similarities calculated from Table 1 by ($100C/N_1$; where C=number of species in common and N_1=number of species in smaller fauna).

	WITTSBURG ROXANA (N=15)	WITTSBURG third loess (N=21)	OLD RIVER section (N=22)	POWDER-MILL CREEK (N=31)
WITTSBURG PEORIA (N=10)	80	80	60	90
WITTSBURG ROXANA (N=15)	--	67	53	73
WITTSBURG third loess (N=21)	--	--	57	59
OLD RIVER SECT. (N=22)	--	--	--	73

Table 3. Faunal similarities calculated from Table 1 by ($100C/N_1$; where C=number of species represented by more than one individual shared in common and N_1=number of species in smaller fauna).

	WITTSBURG ROXANA (N=13)	WITTSBURG third loess (N=19)	OLD RIVER section (N=18)	POWDERMILL CREEK (N=22)
WITTSBURG PEORIA (N=9)	89	100	67	78
WITTSBURG ROXANA (N=13)	--	71	43	50
WITTSBURG third loess (N=19)	--	--	63	63
OLD RIVER SECT. (N=18)	--	--	--	53

macclintocki can be found living in northeastern Iowa. These species, which are common loess fossils in the lower Great Lakes region, have been able to survive locally because of microclimatic conditions generated by cold air draining from snow trapped beneath talus blocks of Niagaran carbonate rocks. North facing slopes, which are kept cool and moist during summer months, permit the area to serve as a refugium for some boreal taxa (Frest and Faye, 1980). The southward range extension of these taxa suggest that they probably lived at a time characterized by slightly cooler summer temperatures. The absence of many of the larger woodland species that are now living in the St. Clair County area indicates that the Powdermill Creek fossils probably lived during a warmer interval (interstadial?) of the Illinoian. This interpretation is supported by the stratigraphic position of the Chinatown silt between the Sangamon and Yarmouth Geosols.

DISCUSSION

Table 2 shows the results of faunal similarity comparisons between the molluscs from the Wittsburg, Old River section and Powdermill Creek. Only taxa identified to the species level in Table 1 have been used in these comparisons. The large number of species represented by single individual occurrences, however, have tended to distort the similarity indices. A second analysis was made (Table 3) which excluded species represented by single individual occurrences. It is assumed that many of these solitary occurrences probably represent reworking from older deposits. The high faunal similarity values shared by the mollus-

Table 4. Comparison of alloisoleucine/isoleucine epimerization ratios for shell from the third loess at Wittsburg Quarry and Chinatown silt at Powdermill Creek.

TAXON	LAB. NUMBER	TOTAL HYDROLYSATE MEAN	S. D.	N	LOCALITY
Anguispira alternata	MSUAGL 93001	0.21	0.03	4	Powdermill-sec B
Hendersonia occulta	MSUAGL 93002	0.16	0.03	3	Powdermill-sec B
Pomatiopsis lapidaria	MSUAGL 93003	0.17	0.02	3	Powdermill-sec B
Pomatiopsis lapidaria	MSUAGL 93004	0.17	0.05	3	Powdermill-sec A
Hendersonia occulta	MSUAGL 93009	0.25	0.05	4	Powdermill-sec B
Hendersonia occulta [a]	AGL 431	0.22	0.02	3	Powdermill-sec A
Hendersonia occulta [b]	MSUAGL 90038	0.22	0.02	2	Wittsburg-3rd loess
Hendersonia occulta [b]	MSUAGL 90098	0.23	0.01	2	Wittsburg-3rd loess
Hendersonia occulta [b]	MSUAGL 90103	0.22	0.00	2	Wittsburg-3rd loess
Hendersonia occulta [b]	MSUAGL 90105	0.30	0.00	2	Wittsburg-3rd loess
Hendersonia occulta [b]	MSUAGL 90107	0.28	0.01	2	Wittsburg-3rd loess
Hendersonia occulta [b]	MSUAGL 90109	0.25	0.02	2	Wittsburg-3rd loess
Hendersonia occulta [b]	MSUAGL 90113	0.30	0.05	2	Wittsburg-3rd loess
Hendersonia occulta [b]	MSUAGL 91098	0.39	0.02	2	Wittsburg-3rd loess

[a] Data from Clark and others, 1989.

[b] Data from Mirecki and Miller,1994

can assemblages from the Peoria, Roxana, and third loess at Wittsburg Quarry (Table 3) suggest the presence of similar environmental conditions at the time the three loess units accumulated. The low faunal similarity between the Illinoian Chinatown silt and third loess (53%) molluscan assemblages, however, is probably a manifestation of local habitat differences reflected by the presence of aquatic taxa in the Powdermill Creek fauna, and probable temperature differences, suggested by the presence *Discus macclintocki*, a relict species now restricted to cold air drainage slopes in northeastern Iowa. In addition, the stratigraphic position of the Chinatown silt at Powdermill Creek, suggests that it may be slightly older than the third loess at Wittsburg Quarry.

Many of the boreal-arctic faunal elements commonly found in the Illinoian and Wisconsinan loess faunas to the north of Crowleys Ridge in Illinois (Leonard and others, 1971; Leonard and Frye, 1960) are missing from the Wittsburg molluscan faunas. They do, however, include several species that are well south of their modern geographic ranges in the Mississippi Valley. A most parsimonious explanation for the southward extension of range of these species would be that they probably lived during times characterized by cooler summer temperatures.

ACKNOWLEDGMENTS

Collection and study of the Powdermill Creek molluscs was in part supported by National Science Foundation grants EAR-8618228 and EAR-8618230. The AMS date from Wittsburg Quarry was funded by a grant from the Division of Research and Graduate Studies, Kent State University. Thanks are extended to Donald McKay, Illinois State Geological Survey who provided the original shell materials collected from the third loess at Wittsburg Quarry and from section "A" at Powdermill Creek for study. We also thank William Miller, whose careful review resulted in changes that have greatly improved the paper. This is contribution number 558, Kent State University, Department of Geology.

REFERENCES CITED

Autin, W.J., Burns, S.F., Miller, B.J., Saucier, R.T., and Snead, J.I., 1991, Quaternary Geology of the lower Mississippi Valley: *in* The Geology of North America v. K-2, Quaternary Nonglacial Geology: Conterminous U.S. *in* (Morrison, R.B., Ed.),p. 547-582. Geological Society of America,

Boulder, CO.

Baker, F.C., 1939, Fieldbook of Illinois Land Snails: State of Illinois Natural History Survey, 166 p.

Burch, J.B. and Jung, Y., 1988, Land Snails of the University of Michigan Biological Station Area: Walkerana, v. 9, p. 1-177.

Clark, P.U., Nelson, A.R., McCoy, W.D., Miller, B.B., and Barnes, D.K., 1989, Quaternary Aminostratigraphy of Mississippi Valley Loess: Geological Society of America Bulletin, v. 101, p. 918-926.

Clarke, A. H., 1981, The Freshwater Molluscs of Canada: National Museum of Canada, Ottawa. 446 p.

Dundee, D.S., 1957, Aspects of the Biology of *Pomatiopsis Lapidaria* (Say) (Mollusca: Gastropoda: Prosobranchia): University of Michigan, Museum of Zoology, Miscellaneous Publications, no. 100, 65 p.

Frest, T.J. and Fay, L. P., 1980, Relict land snails from the Driftless area, Iowa, with implications for Pleistocene climates: Geological Society of America Abstracts with Programs v. 12, p. 49.

Hubricht, L., 1985, The Distribution of the native land mollusks of the Eastern United States: Fieldiana, Zoology, new series, No. 24, p. 1-191.

Jokinen, E.H., 1992, The freshwater snails (Mollusca: Gastropoda) of New York State: New York State Museum Bulletin no. 482, 112 p.

Leonard, A.B., Frye, J.C., and Johnson, W.H., 1971, Illinoian and Kansan faunas in Illinois: Illinois State Geological Survey, Circular, no. 461, p. 1-23.

Leonard, A.B. and Frye, J.C., 1960, Wisconsinan molluscan faunas of the Illinois Valley region: Illinois State Geological Survey Circular no. 304, p. 1-32.

McKay, E.D., 1989, Illinoian and older loesses and tills at the Marysville section: Illinois State Geological Survey Guidebook 23, p. 21-30.

Mirecki, J.E. and Miller, B.B., 1994, Aminostratigraphic correlation and geochronology of two Quaternary loess localities, Central Mississippi Valley: Quaternary Research, v. 41 (3).

Parks , W.S. and Loundsbury, R.W., 1975, Environmental geology of Memphis, Tennesse: *in* Field Trips in western Tennessee. Report of Investigations no. 36. (R.G. Stearns, Ed.,) p. 35-51. Tennessee Division of Geology, Nashville, TN.